WELLINGTON FIELD

MISSISSIPPIAN FORMATION

Preliminary Reservoir Description

(Permeability, Capillary Pressure, and Relative Permeability)

Prepared by:
Mohsen Fazel Alavi, Mina Fazel Alavi, and Maryam Fazel Alavi

November 13, 2012

Kansas Geological Survey Open-File Report 2015-26

Table of Contents

List of Figures

List of Tables

Appendix A

Appendix B

Appendix C

I- Introduction

In order to facilitate 3D dynamic modeling of the reservoir, this paper seeks to describe and characterize Mississippian formation in the Wellington Field. Based on available data, permeability in wells without core is estimated, and capillary pressure curves and relative permeability curves are proposed for different rocks in the reservoir. Existing data in the field has been used in reservoir characterization, and when the necessary data were missing generalized correlations from the same formation and other fields were utilized.

The Wellington Field is located in southern Kansas, Sumner County (T 31S-R1W). The Mississippian formation, based on lithology, can be divided from top to bottom, into 3 lithofacies sequences: chat conglomerate, dolomitic sequence, and carbonate interval at the bottom. The field is very old; it was discovered and put into production in 1929. Later, water injection was started in 1953. Oil production has been continued to the present time. Available data mainly consist of very old neutron logs with or without resistivity logs. New wells have modern suites of logs and recently drilled wells have, in addition, NMR data. This section provides a brief description of available data for the field.

There are 16 wells with complete suites of porosity and resistivity logs available in sections 28, 29, 32, and 33 drilled from 1956 to 2011. Also, there were five older wells with older completion dates from 1936 to 1948. These wells had one porosity log, usually neutron logs with no scale or counts/API units. Resistivity logs were not recorded in these wells. The neutron logs of the five older wells were normalized with the neutron logs of the key well (1-32) and then converted to the equivalent formation porosity using Well 1-32. Therefore, formation porosity from these five old wells may not be reliable. The 16 newer wells were quality controlled and analyzed by Techlog in terms of porosity, water, oil saturation, and minerals. Two of these 16 wells (1-32 and 1-28) had NMR logs. The NMR logs were analyzed by Techlog to derive Coates permeability and Pc curves. Only Well 1-32 and Peasel 1 had core data. These core data had porosity, permeability (90 degree and maximum), and matrix density. Based on the production history of the field, the field production started in 1929 without any significant water production prior to 1943. Newer wells were drilled after this date and must be invaded by formation water or water flood. Therefore, water saturation derived from Techlog using resistivity logs is not representative of initial water saturation of the reservoir. Moreover, the older wells didn't have any resistivity logs; therefore, initial water saturation couldn't be derived from resistivity logs.

Well 1-32 has the most complete set of data and was used as the key well. Routine core data of this well was analyzed by FZI method, and FZI was correlated with log-derived porosity and water saturation of this well (NMR irreducible water saturation). Based on irreducible water saturation and porosity, permeability in Well 1-32 was estimated, which matched very well with core data. Since initial water saturation was not available in other wells to be converted to irreducible water saturation to find permeability, permeability of these wells were estimated by another technique. The reservoir was divided into six zones based on log signatures and FZI, and then the permeability of each zone was estimated.

In the absence of special core analysis data, NMR data of Well 1-32 were used to derive capillary pressure curves for different zones of the reservoir. However, these Pc curves are not presented in this

paper and will be discussed in a separate report. Pc curves in this report are based on generalized Pc curves and NMR irreducible water saturations. Also core relative permeability data were missing. Based on estimated end points from Well 1-32 and generalized data from other fields, relative permeability curves were generated for all rock types. Since special core analyses is being performed in the lab on core samples of Well 1-32, proposed capillary pressure curves and relative permeability curves in this report will be calibrated against lab data in the future.

II- Permeability Determination

a. Analysis of Data from Well 1-32 (Key Well)

i. Log Analysis

Conventional and geochemical logs of this well were analyzed by TechLog to determine minerals, porosity, and water saturation as presented in fig. A1 (Appendix A). It should be noted that calculated water saturation might not represent initial water saturation because of field production history.

ii. Routine Core Data

Routine core analysis data consisting of porosity, permeability (max, 90 degree), and matrix density were available in this well for the interval 3,627.55 to 5,176.25 ft, which covers the Mississippian and Arbuckle formation. Core data were analyzed by FZI method and six discrete rock types (RT) were defined in the Mississippian reservoir (fig. 1). Each RT has a specific permeability-porosity correlation, which is shown in fig 1. Equation 1 was used to calculate the Reservoir Quality Indicator (RQI) and was used in equation 2 to calculate FZI:

$$RQI = 0.0314\sqrt{\frac{K}{\phi_e}} \qquad \text{(Equation 1)}$$

$$\mathrm{FZI} = \frac{\mathrm{RQI}}{\phi_z} \qquad \text{(Equation 2)}$$

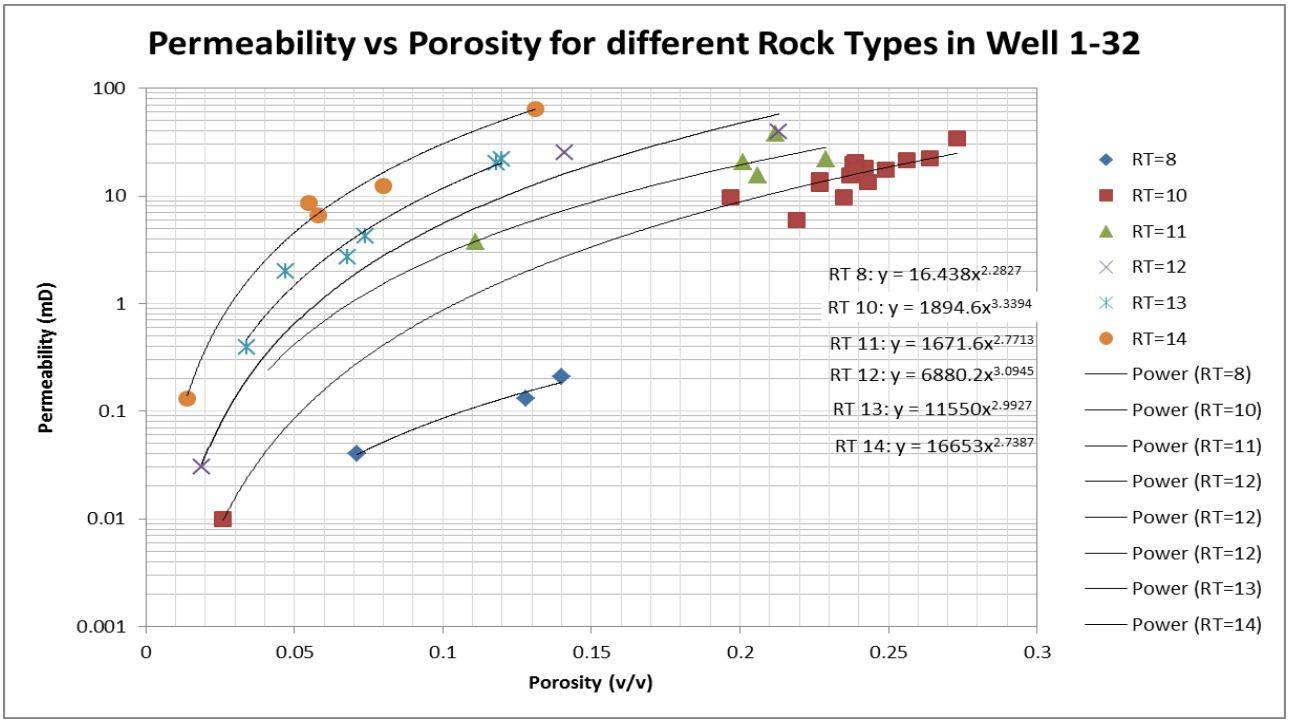

Figure 1: Permeability vs. porosity for different rock types in Well 1-32

The RQI of these core samples are plotted versus normalized porosity in fig. 2 below. Each RT has a specific FZI (intercept of the straight line with RQI axis, where normalized porosity is 1). If FZI in other wells could be determined, equations in fig. 1 could be used to calculate permeability in other wells.

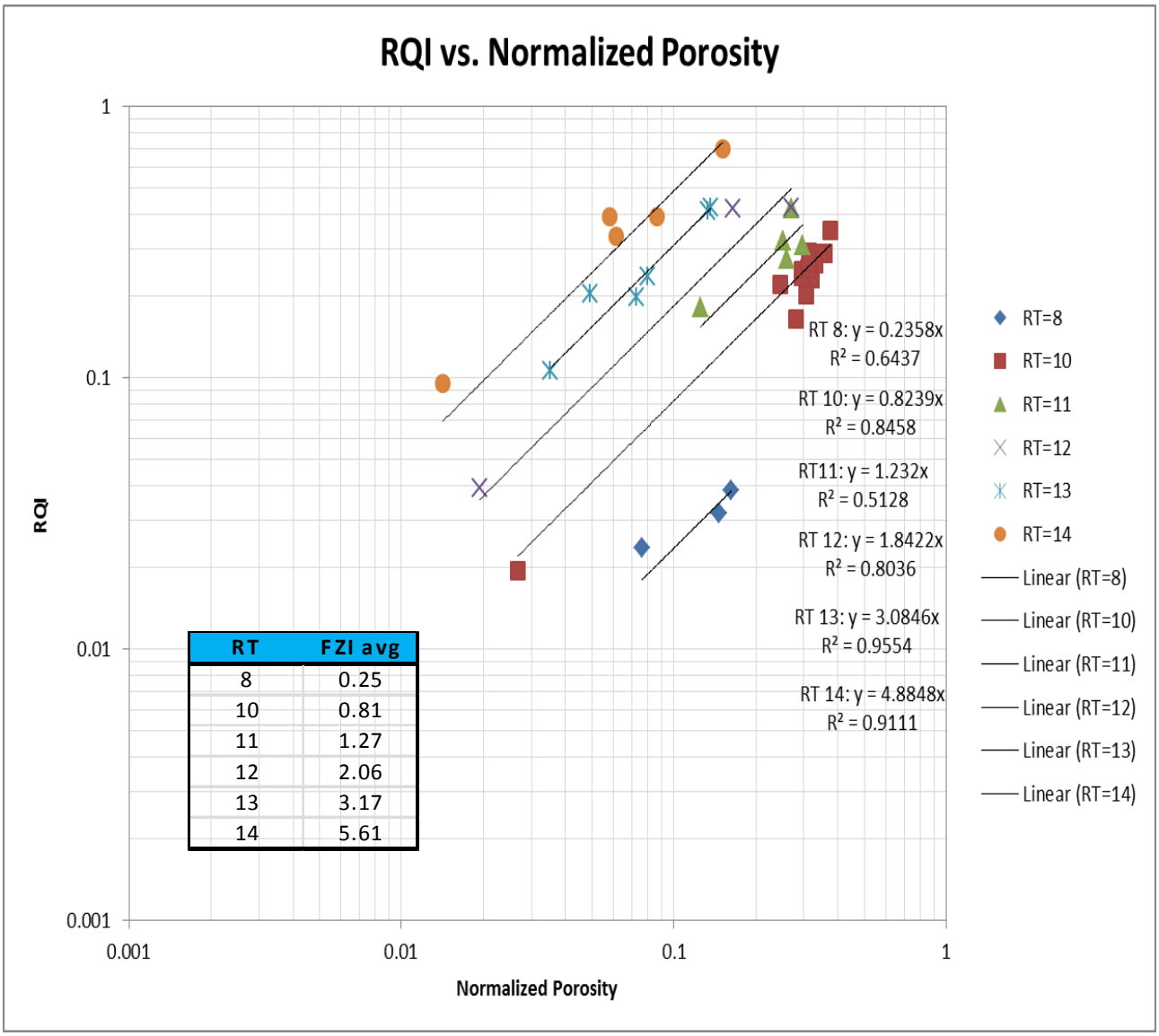

RT	FZI avg
8	0.25
10	0.81
11	1.27
12	2.06
13	3.17
14	5.61

Figure 2: RQI vs. normalized porosity for different rock types in Well 1-32

It has been found that FZI is related to the reciprocal of porosity and irreducible water saturation. FZI has been related by others to log signatures in the key well and a correlation is found between FZI and log signatures, which are then used to find FZI in other wells. This method was not used in this report because often it doesn't give accurate results.

As will be discussed below, FZI from core will be related to irreducible water saturation from NMR to find permeability equations based on reservoir porosity and water saturation, which can be used when irreducible water saturation is known.

iii. NMR Log Results

The NMR log was analyzed by TechLog to derive porosity, irreducible water saturation at Pc equal to 20 bar (290 psi), entry pressure, and capillary pressure. Also initial water saturation based on FWL and densities of formation water and oil were obtained. These parameters and Kappa values, which were used in NMR interpretation, are given below:

Parameters and Kappa values used in NMR interpretation

Free water Level: -2,494 (ft)

Interfacial tension of oil-water: 20 (dyne/cm)

Water density: 1.11 (g/cm3)

Oil density: 0.83 (g/cm3)

Kappa in chat and carbonate: 9 and 15 (psi.s)

Kappa low in chat and carbonate: 5 and 5 (psi.s)

Kappa flex point in chat and carbonate: 20 and 100 (ms)

The results of the interpretation are shown in figs. A2 and A3 (Appendix A).

b. Permeability of Well 1-32

Permeability of this well can be obtained by different methods and different sources of data. The basic permeability data source is routine core analysis, which was discussed above. Another method is Coates equation (equation 3), which relates permeability to porosity, FFI, and BWT:

$$K_{Coates} = A * (10 * \phi)^B * \left(\frac{FFI}{BWT}\right)^C \quad \text{(Equation 3)}$$

Coates permeability was calculated using FFI and BWT from NMR; however, different A pre-factors in the above equation were used in different intervals of the reservoir to match Coates permeability with core permeability.

The reservoir was divided into three intervals and the following pre-factors were applied.

- Zone 1: from 3,658 to 3,668 ft, A= 4.5
- Zone 2: from 3,668 to 3,720 ft, A=0.8
- Zone 3: from 3,720 to 4,100 ft, A=3

Coates permeability is compared with core data in fig. A4 (Appendix A). The match between Coates permeability and core data is acceptable but not perfect. In addition, permeability of this well can be

obtained from irreducible water saturation and porosity of the well using equation 4, when constants ***a*** and ***b*** are known. This equation was derived by the lead author.

$$K = 1014\left[\frac{a}{S_{wir}\phi_e} + b\right]^2 \frac{\phi_e^3}{(1-\phi_e)^2} \qquad \text{(Equation 4)}$$

Constants ***a*** and ***b*** in the above equation can be found by relating FZI to $\frac{1}{S_{wir}\cdot\phi_e}$ as follow:

$$FZI = \frac{a}{S_{wir}\phi_e} + b \qquad \text{(Equation 5)}$$

For this purpose, FZI from core was statistically related to the reciprocal of porosity and irreducible water saturation from NMR. To find the right constants, the reservoir interval had to be divided into two zones, A and B. Zone A is mainly the chat conglomerate sequence, which has bimodal T2 distributions; the dolomite and limestone sections below the chat conglomerate, generally, have single modal pore size distribution (fig. A3—Appendix A) (zone A and B). Due to changes in T2 distribution shape, two correlations were necessary. The first correlation is derived for zone A (chat conglomerate), which is shown in fig. 3 and equation 6.

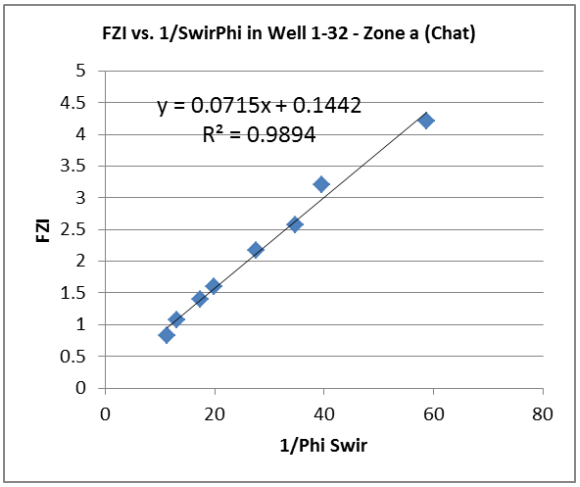

Figure 3: FZI vs. 1/PhiSwir for zone A (chat)

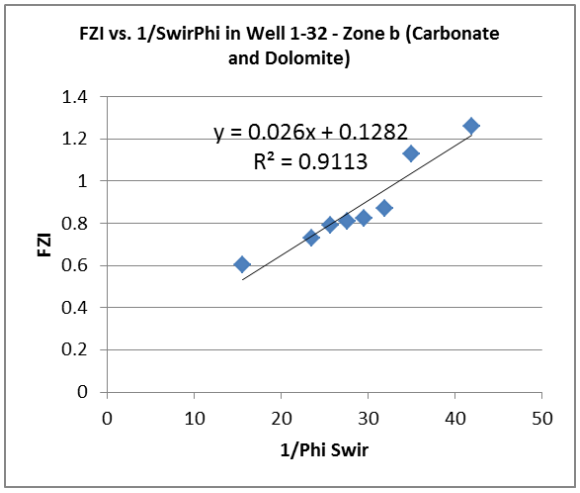

Figure 4: FZI vs. 1/PhiSwir for zone B (dolomite and carbonate)

The permeability equation for zone A is givenin equation 7. Equation 5 is the Tiab equation, where FZI is replaced by irreducible water saturation and porosity.

$$\mathrm{FZI_{ZoneA}} = \frac{0.0715}{\mathrm{S_{wir}\phi_e}} + 0.1442 \qquad \text{(Equation 6)}$$

$$\mathrm{K} = 1014\left[\frac{0.0715}{\mathrm{S_{wir}\phi_e}} + 0.1442\right]^2 \frac{\phi_e^3}{(1-\phi_e)^2} \qquad \text{(Equation 7)}$$

For zone B, the correlation between FZI and $\frac{1}{S_{wir}.\phi_e}$ is obtained and illustrated in fig. 4. Substituting FZI in the Tiab equation by this correlation, the following permeability equation (equation 9) for zone B is obtained.

$$FZI_{ZoneB} = \frac{0.026}{S_{wir}\phi_e} + 0.1282 \qquad \text{(Equation 8)}$$

$$K = 1014\left[\frac{0.026}{S_{wir}\phi_e} + 0.1282\right]^2 \frac{\phi_e^3}{(1-\phi_e)^2} \qquad \text{(Equation 9)}$$

Equations 7 and 9 were applied respectively to zones A and B of Well 1-32 and permeability log versus depth was generated. Permeability by this method matches better with core data as shown in fig. A4 (Appendix A). This method could, easily, be applied to all of the wells in the field if reliable initial water saturation and porosity existed. Initial water saturation data can be converted to irreducible water saturation by a method that will be discussed in a paper to be published. However, in the Wellington Field, application of this method to other wells is not practical due to lack of reliable initial water saturation due to logging after a long period of water flooding of the Mississippian reservoir.

c. Permeability in Well 1-28

Well 1-28 has NMR log data, and two methods can be used to determine its permeability. Coates permeability in this well was obtained using the same **A** factors that were used in Well 1-32. Permeability was also found for this well based on assigned FZI values, based on engineering judgement, to different zones of the reservoir and calculation of permeability by the Tiab equation. The method of assigning FZI will be discussed in the next section.

Coates permeability is compared with FZI permeability in fig. A11 (Appendix A), where there is a better match between FZI permeability with core data.

d. Equivalent FZI Zones in Other Wells Corresponding to Well 1-32 FZI

Equations 7 and 9 could be used for permeability determination in all of the wells, if reliable initial water saturation existed in these wells (initial water saturation can be converted to irreducible water saturation by Pc equations). This method could not be used effectively in this case because log-based water saturations are generally affected by oil production from the reservoir and water injection in the reservoir. Another method, which has often been used and is described in the literature, is relating FZI from core in the key well with log signatures through regression or Neural Network and subsequent application of the resulting correlation to other wells with similar logs. It is doubtful that this process gives accurate results in the Mississippian formation because, generally, wells are old and do not have high-quality logs. In addition, the method works better if a deep resistivity log is included in regression analysis for correlation determination. However, in this field, deep resistivity in Well 1-32 and other wells is affected by production or water injection.

Another method is proposed, which is not ideal and is not theoretically correct but which might provide the best possible permeability model for predicting permeability based on the existing data.

Comparison of T2 distribution, before hydrocarbon correction, in Well 1-32 and Well 1-28, shows that there are intervals with similar shape and size of pore in both of the wells. It is concluded that tortuosity, shape factor of grains and surface area per grain volume are similar in both wells in co-relatable intervals. Therefore, it can be said that zones of equal FZI exist in both of the wells.

FZI values of Well 1-32 are plotted versus depth in fig. A4 (Appendix A). Study of FZI variation with depth indicates that the reservoir can be divided into six zones (3 zones in chat and 3 zones in the carbonate interval), each zone with a distinct average FZI. These zones are shown in fig. A5 (Appendix A) and table 1:

Table 1: Average FZI in six zones of Well 1-32

Zone	from (ft)	to (ft)	FZI (µm)
1	3,656	3,659	2.605
2	3,659	3,662.5	1.618
3	3,662.5	3,665.5	4.285
4	3,665.5	3,698.5	1.007
5	3,698.5	3,720	0.476
6	3,720	3,766	0.925

It is assumed that equivalent zones with equal FZI value exist in other wells, which can be defined by log correlation. Porosity, density, and GR logs of the wells were used to find equivalent zones in other wells corresponding to six zones of Well 1-32. Well cross sections of figs. A6–A10 (Appendix A) show boundaries of the zones in other wells. FZI values in table 1 were assigned to respective zones in other wells and a permeability log was generated, as will be discussed below.

e. Permeability in Well Peasel 1

Well Peasel 1 had core data, which are plotted in fig. A12 (Appendix A). Average FZI values from Well 1-32 were assigned to equivalent zones in well Peasel 1, and permeability of this well was calculated based on assigned FZI values using the Tiab Equation (equation 10). The calculated permeability is also plotted in fig. A12 (Appendix A) and is compared with core permeability. There is a good match between the derived permeability using FZI and core data.

f. Permeability in Other Wells

It was assumed that each zone in figs. A6–A10 (Appendix A) had a specific FZI value; these are listed in table 1. This assumption is approximately but not theoretically correct and may give a good estimate of

permeability in other wells, where no other viable and more accurate method exists. Based on FZI of each zone and effective porosity of the wells, the permeability of all zones in all wells was calculated using the Tiab equation (equation 10).

$$K = 1014\ FZI^2 \frac{\phi_e^3}{(1-\phi_e)^2} \qquad \text{(Equation 10)}$$

Although there was a good match between calculated permeability by this method in well Peasel 1 with core permeability, it is admitted that the predicted permeability in other wells, except for Well 1-32 and Well 1-28, are not ideal. However, considering the available data, it is believed it is the best that could be estimated. Calculated permeability data of wells are shown in Figs. A11 to A25 (Appendix A).

The obtained permeability data can be used in the construction of the dynamic model of the reservoir. During history matching of the dynamic model, when there is mismatch, permeability of the well can be multiplied by a factor to obtain the desired match between actual production data and simulation results. By this procedure, model permeability could be improved.

III- Capillary Pressure Curves

Dynamic modelling of the Mississippian reservoir needs capillary pressure curves. Available data for determination of Pc curves are generalized Pc curves for the Mississippian formation, NMR data of Well 1-32 and Well 1-28. Data used to generate Pc curves for both chat and carbonate sequences of this reservoir were drawn mainly from key well (Well 1-32). The shape of the generalized Pc curves was also used in the process.

Often Pc curves are related to the permeability of the rock or the FZI in the literature, while in geological sedimentary environments, different Pc curves could exist for a single permeability or a specific FZI. Investigation by M.F. Alavi has shown that entry pressure, irreducible water saturation and therefore the Pc curve of a rock are related to its Reservoir Quality Index (RQI). In this section, using data of the key well and generalized data, Pc curves are defined for different RQI values in the Mississippian formation. Since permeability in all wells against depth is found according to Section I of this report, RQI at each depth can be determined and Pc curves based on RQI can be applied to all wells to find initial water saturation. Often the grid of the dynamic or static model of the reservoir is divided into several saturation regions, each with a specific RQI. Pc curves and relative permeability tables are prepared for each region.

Both drainage and imbibition Pc curves were calculated for the reservoir. Depending on the path of oil migration into the Mississippian formation, either drainage or imbibition Pc curves could be applied to the model and wells to represent the initial condition of the reservoir.

a. Capillary Pressure Equations

When oil is migrated from the side of the reservoir to the top of the structure and then downwards to the spill point, initial water saturation is described by drainage capillary pressure curves. In some reservoirs, based on log data, it seems that oil migration has been from below of oil water contact (OWC) to the top of the reservoir and all over the reservoir area. In these cases, there is residual oil saturation below OWC, as indicated by log saturations. When oil has migrated from the bottom of the OWC to the top, imbibition Pc curves are more appropriate for description of the initial water saturation.

To determine drainage initial water saturation (Swi), equation 11—a function of irreducible water saturation (Swir) and non-wetting phase (oil) normalized saturation (Snwn)—is proposed.

$$S_{wi} = 1 - S_{nwn}(1 - S_{wir}) \quad \text{(Equation 11)}$$

Snwn is a function of EQR (equivalent radius) (equation 12). Constants *a* and *b* in this equation will be found from the shape of generalized Pc curves later.

$$S_{nwn} = (1 - aEQR)(1 - EQR^b) \quad \text{(Equation 12)}$$

EQR depends on entry pressure and capillary pressure (equation 13), where entry pressure is a function of RQI, which will be derived from the NMR log of Well 1-32.

$$EQR = \frac{P_e}{P_c} \quad \text{(Equation 13)}$$

An equation similar to equation 11 (equation 14) is proposed for imbibition initial saturation determination at different capillary pressures. Equation 14 includes residual oil saturation (Sor). A correlation between Sor and RQI will be proposed later and can be substituted in equation 14

$$S_{wi} = 1 - S_{0r} - S_{nwn}(1 - S_{wir} - S_{or}) \quad \text{(Equation 14)}$$

In the following sections, the initial water saturation equations described above will be expressed in terms of RQI and capillary pressure, and several Pc curves will be generated for both drainage and imbibition conditions. Each Pc curve is for a certain narrow range of rock RQI.

b. Irreducible Water Saturation

There is a good correlation between irreducible water saturation of reservoir rocks and RQI. Irreducible water saturation of special core analysis (SCAL)data and water saturations determined from log suites in other fields, mainly carbonate reservoirs, have indicated that irreducible water saturation at certain capillary pressure can be correlated, very well, to the RQI of the rock. In literature, irreducible water saturation often is correlated to permeability, porosity, or FZI, which is not theoretically a correct methodology. In the Mississippian reservoir, reliable initial water saturation from logs (which could be converted to irreducible water saturation) was not available. However, NMR data from two of the wells can provide irreducible water saturation in these wells.

NMR data of Well 1-32 was used to determine the irreducible water saturation at a Pc of 20 bars (290 psi). Also interfacial tension between oil and water was entered in the Tech-Log Module to find Swir versus depth for this well. Previously, permeability of the Mississippian in Well 1-32 was determined by equation 7 and equation 9. Based on porosity and calculated permeability of Well 1-32, the RQI in this well was determined. Figure 5 plots the irreducible water saturation in Well 1-32 in the chat conglomerate against RQI.

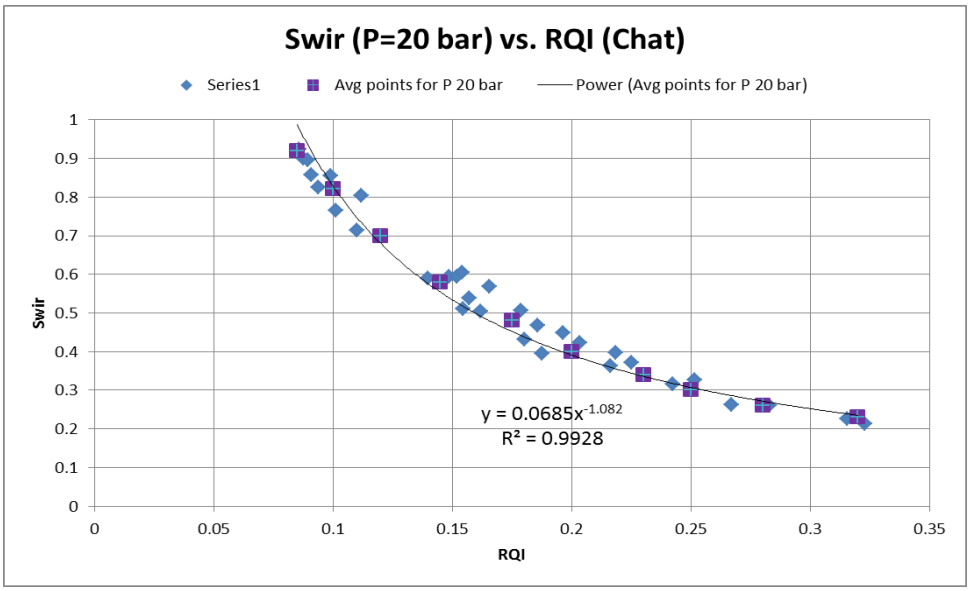

Figure 5: Swir vs. RQI for zone A (chat)

Equation 15 was determined from Figure 5 that is the relationship between Swir and RQI, where R2 is equal to 0.99, indicating good correlation.

$$S_{wir} = 0.0685RQI^{-1.082} \qquad \text{Equation 15}$$

The same procedure was repeated for the carbonate section of the Mississippian formation. Figure 6 is the plot of Swir vs. RQI for this section:

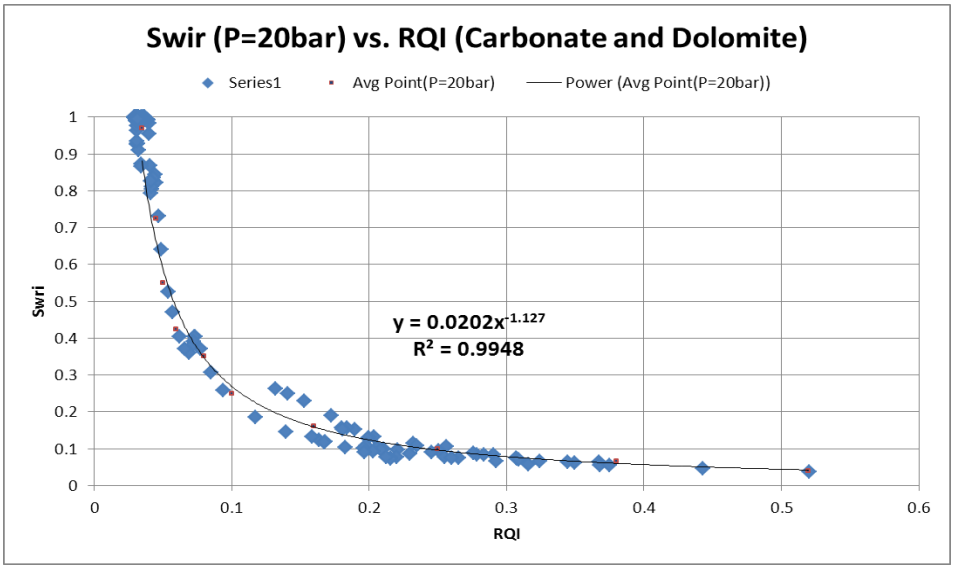

Figure 6: Swir vs. RQI for zone B (carbonate and dolomite)

Equation 16 can be used to determine Swir for the carbonate section.

$$S_{wir} = 0.0202RQI^{-1.127} \qquad \text{Equation 16}$$

c. Entry Pressure

Based on SCAL data from other fields, a good correlation can be found between capillary entry pressure and RQI. Entry pressure in Well 1-32 was determined from NMR data using oil and water interfacial tension. In the Mississippian formation, two correlations were obtained: one for the chat conglomerate and another for the carbonate section of this formation. Figure 7 plots entry pressure from the NMR against RQI in the chat conglomerate.

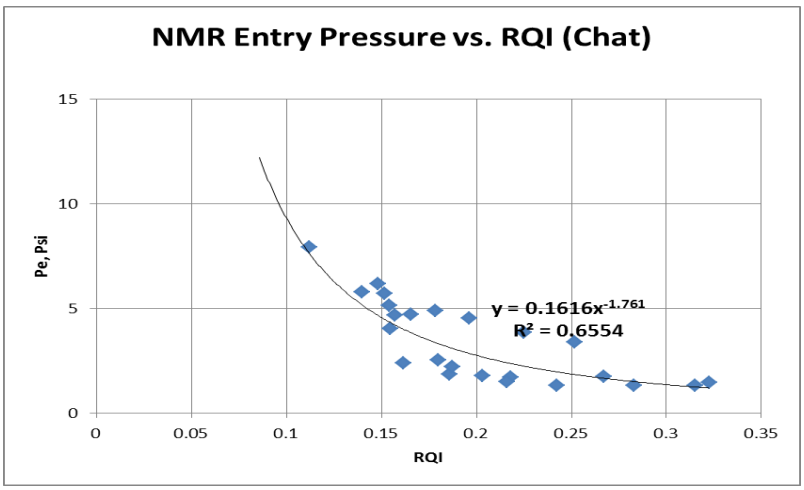

Figure 7: Entry pressure vs. RQI in zone A (chat)

The following equation shows that entry pressure is a function of RQI in the chat conglomerate.

$$P_e = 0.1616RQI^{-1.761} \quad \text{(Equation 17)}$$

Also, fig. 8 plots entry pressure versus RQI in the carbonate section . This plot results in equation 18, which relates entry pressure in this section with RQI.

$$P_e = 0.1467RQI^{-1.312} \quad \text{(Equation 18)}$$

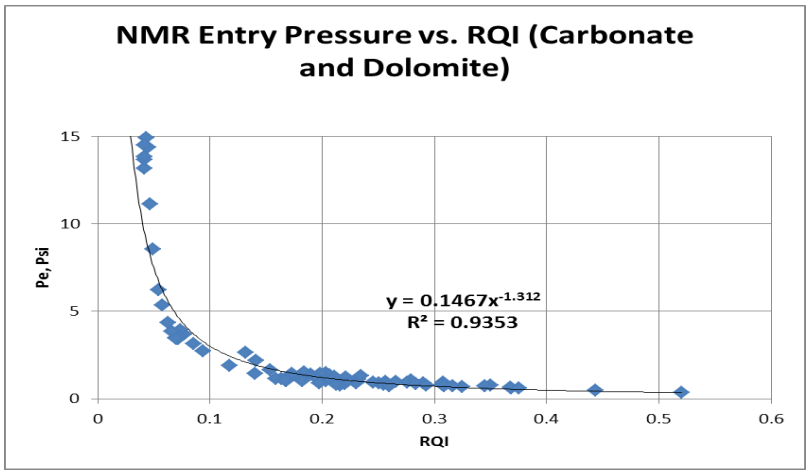

Figure 8: Entry pressure vs. RQI in zone B (carbonate and dolomite)

d. Residual Oil Saturation

A correlation between residual oil saturation and RQI is necessary to enable derivation of imbibition capillary pressure curves. Reliable SCAL data for the Mississippian formation are not available at the present time to drive this correlation. In the absence of such data, the following correlation is suggested for the carbonate section. The correlation has been derived based on SCAL data of other reservoirs and modified for this field.

$$1 - S_{or} = 0.5811RQI^{-0.139} \quad \text{(Equation 19)}$$

For the chat section of the Mississippian formation, the equation for the residual oil saturation has been adjusted to the following:

$$1 - S_{or} = 0.427RQI^{-0.407} \quad \text{(Equation 20)}$$

e. Normalized Non-wetting Phase Saturation (Snwn)

Normalized non-wetting phase (oil) saturation is defined according to equation 21 for drainage initial water saturations. It can be related to EQR by plotting Snwn from Pc curves versus EQR and fitting equation 12 into the plotted data.

$$S_{nwn} = \frac{1-S_{wi}}{1-S_{wir}} \quad \text{(Equation 21)}$$

Generally a single relationship is obtained for all Pc curves from a single sedimentary environment where pore size distribution does not change. In the Mississippian reservoir, two Snwn correlations were obtained using published generalized Pc curves.

Figure 9 shows the generalized Pc curves of the chat conglomerate in the Mississippian in the Spivey-Grabs field (Watney et al., 2001). First, Pc curves were extrapolated to 300 psi to find irreducible water saturation.

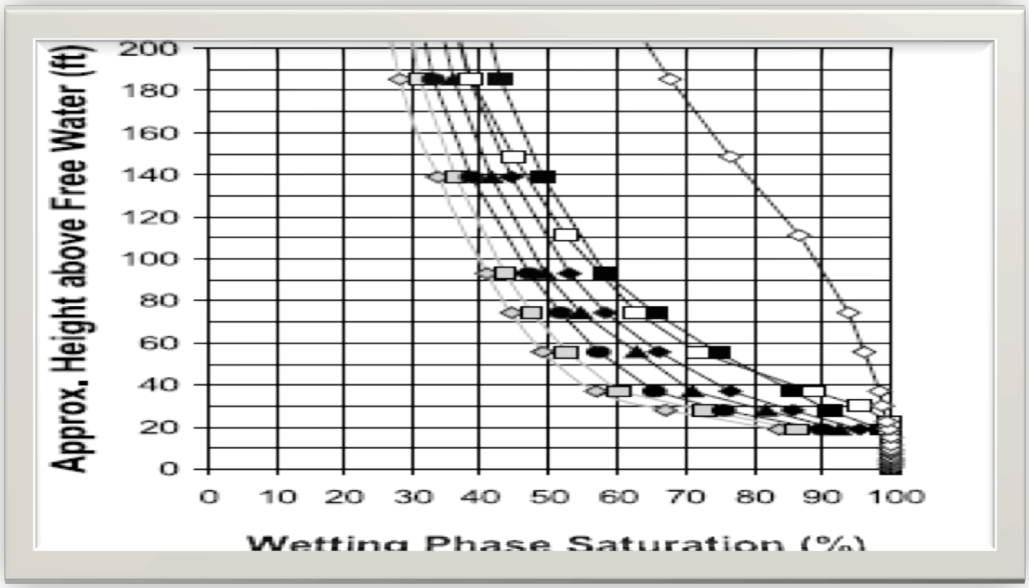

Figure 9: Generalized Pc curves (height above free water) for permeability groups in Spivey-Grabs Field Mississippian chat

Snwn was calculated for several water saturations along the curves and plotted against respective EQR, fig. 10.

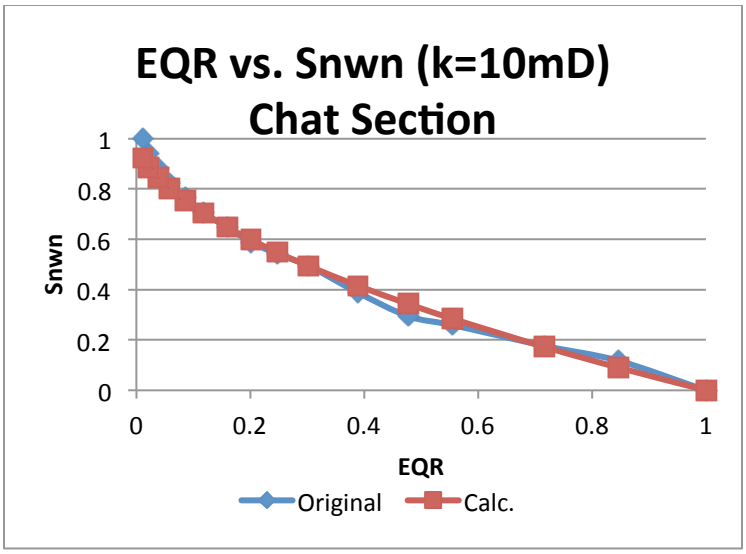

Figure 10: Snwn vs. EQR for chat section at K=10mD

Constants *a* and *b* of equation 12 were derived by regression and resulted in the following equation for the chat conglomerate of this reservoir.

$$S_{nwn} = (1 - 0.00155EQR)(1 - EQR^{0.5697}) \qquad \text{(Equation 22)}$$

Figure 11 shows the generalized Pc curves for the carbonate zone of the Mississippian reservoir (Bhattacharya et al., 2003).

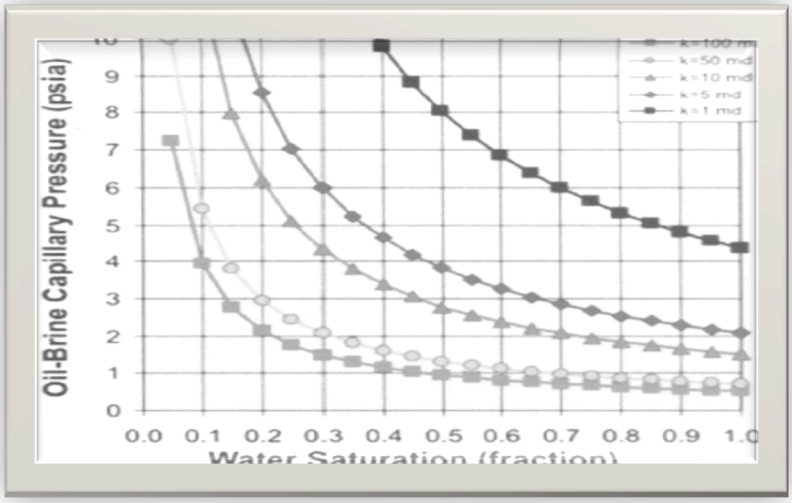

Figure 11: Generalized Pc curves for permeability groups in the Mississippian carbonate section

The curves above were used to find the correlation between Snwn and EQR in the carbonate section, fig. 12 and equation 23.

$$S_{nwn} = (1 - 0.5245EQR)(1 - EQR^{3.1249}) \quad \text{(Equation 23)}$$

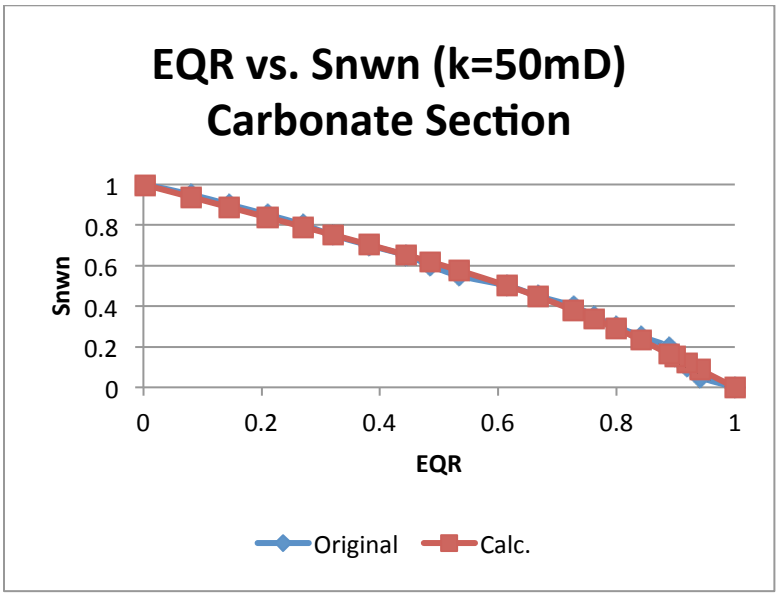

Figure 12: Snwn vs. EQR for the carbonate section at K=50mD

f. Calculation of Drainage Capillary Pressure Curves

Equation 11 was proposed for drainage water saturation. According to equation 11, initial water saturation (Swi) is a function of Swir and Snwn. It was shown that irreducible water saturation is a function of RQI (equations 15 and 16) and Snwn is a function of RQI and Pc (equations 22 and 23). Swir and Snwn in equation 11 can be replaced by respective functions and an equation can be obtained that expresses Swi in terms of RQI and Pc.

For the chat conglomerate, equations 15 and 22 were incorporated into equation 11 to obtain equation 24, which gives water saturation for every Pc and RQI.

$$S_{wi} = 1 - \left(1 - 0.0015\frac{0.1616RQI^{-1.761}}{P_c}\right)\left(1 - \left(\frac{0.1616RQI^{-1.761}}{P_c}\right)^{0.569}\right)(1 - 12.885RQI^2 + 8.031RQI - 1.4924) \quad \text{(Equation 24)}$$

It was decided to calculate eight capillary pressure curves for the chat conglomerate to be used in the reservoir model. RQI in chat ranges from 0.108 to 0.340. This range was divided into eight subdivisions (table 2).

Table 2: Subdivisions of RQI range in chat section

RT	From	To	Avg RQI
1	0.300	0.340	0.320
2	0.265	0.300	0.280
3	0.240	0.265	0.250
4	0.215	0.240	0.230
5	0.188	0.215	0.200
6	0.160	0.188	0.175
7	0.133	0.160	0.145
8	0.108	0.133	0.120

The mid-range of each subdivision was used to calculate eight Pc curves (equation 24, table 3). The generated Pc curves are shown in fig. 13. These curves are in agreement with generalized curves, when the right permeability and RQI are considered and compared.

Table 3: Drainage Pc table for different RQI groups in the Mississippian chat

a 0.0016	b 0.570	Drainage Table in Mississippian Chat						
RQI	0.32	0.28	0.245	0.22	0.2	0.175	0.145	0.12
Pe	1.20	1.52	1.92	2.33	2.75	3.48	4.84	6.76
Swir	0.23	0.26	0.3	0.34	0.4	0.48	0.58	0.7
Pc	**Swi**							
0	1.00	1.00	1.00	1.00	1.00	1.00	1.00	1.00
0.1	1.00	1.00	1.00	1.00	1.00	1.00	1.00	1.00
0.2	1.00	1.00	1.00	1.00	1.00	1.00	1.00	1.00
0.3	1.00	1.00	1.00	1.00	1.00	1.00	1.00	1.00
0.4	1.00	1.00	1.00	1.00	1.00	1.00	1.00	1.00
0.5	1.00	1.00	1.00	1.00	1.00	1.00	1.00	1.00
0.6	1.00	1.00	1.00	1.00	1.00	1.00	1.00	1.00
0.7	1.00	1.00	1.00	1.00	1.00	1.00	1.00	1.00
0.8	1.00	1.00	1.00	1.00	1.00	1.00	1.00	1.00
0.9	1.00	1.00	1.00	1.00	1.00	1.00	1.00	1.00
1	1.00	1.00	1.00	1.00	1.00	1.00	1.00	1.00
2	0.806	0.893	0.985	1.00	1.00	1.00	1.00	1.00
3	0.687	0.763	0.844	0.911	0.971	1.00	1.00	1.00
4	0.618	0.687	0.761	0.825	0.885	0.960	1.00	1.00
5	0.572	0.636	0.706	0.767	0.827	0.903	0.993	1.00
6	0.538	0.599	0.666	0.725	0.785	0.861	0.952	1.00
8	0.492	0.547	0.611	0.667	0.727	0.804	0.896	0.973
10	0.460	0.513	0.574	0.628	0.688	0.765	0.858	0.940
12	0.438	0.488	0.547	0.599	0.659	0.737	0.831	0.916
14	0.420	0.469	0.526	0.577	0.637	0.715	0.810	0.898
20	0.385	0.431	0.484	0.534	0.594	0.672	0.767	0.862
30	0.353	0.395	0.446	0.494	0.554	0.632	0.729	0.828
40	0.335	0.375	0.424	0.471	0.531	0.609	0.706	0.809
50	0.322	0.361	0.409	0.455	0.515	0.594	0.691	0.796

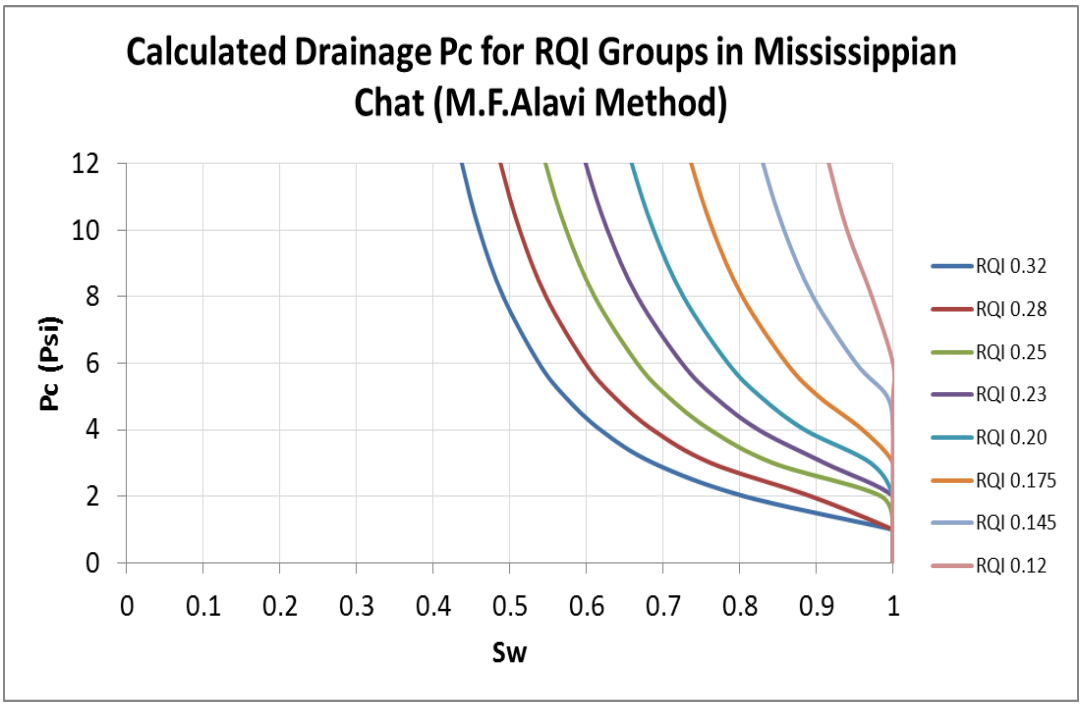

Figure 13: Calculated drainage Pc curves for the Mississippian chat

For the carbonate section of the reservoir, equations 16 and 23 were integrated into equation 11 to obtain an equation expressing Swi in terms of RQI and Pc (equation 25).

$$S_{wi} = 1 - \left(1 - 0.5245 \frac{0.1467 RQI^{-1.312}}{P_c}\right)\left(1 - \left(\frac{0.1467 RQI^{-1.312}}{P_c}\right)^{3.125}\right)(1 - 0.0202 RQI^{-1.127})$$

(Equation 25)

The RQI in the carbonate section ranges from 0.045 to 0.590. The range was divided into eight smaller intervals (table 4). The midpoint of each range was found and, based on these RQI values, eight Pc curves were calculated for the carbonate section of the reservoir (table 5 and fig. 14).

Table 4: RQI subdivisions in the Mississippian carbonate

RT	From	To	Avg RQI
1	0.450	0.590	0.520
2	0.315	0.450	0.380
3	0.205	0.315	0.250
4	0.130	0.205	0.160
5	0.090	0.130	0.100
6	0.070	0.090	0.080
7	0.055	0.070	0.060
8	0.045	0.055	0.050

Table 5: Drainage Pc table for different RQI groups in the Mississippian carbonate

a 0.524	b 3.125	Drainage Table in Mississippian Carbonate						
RQI	0.52	0.38	0.25	0.16	0.1	0.08	0.06	0.05
Pe	0.346	0.522	0.904	1.624	3.009	4.033	5.882	7.471
Swir	0.04	0.065	0.1	0.16	0.25	0.35	0.425	0.55
Pc	**Swi**							
0	1	1	1	1	1	1	1	1
0.1	1	1	1	1	1	1	1	1
0.2	1	1	1	1	1	1	1	1
0.3	1	1	1	1	1	1	1	1
0.4	0.809	1	1	1	1	1	1	1
0.5	0.582	1	1	1	1	1	1	1
0.6	0.450	0.821	1	1	1	1	1	1
0.7	0.367	0.658	1	1	1	1	1	1
0.8	0.312	0.547	1	1	1	1	1	1
0.9	0.272	0.468	1	1	1	1	1	1
1	0.243	0.410	0.872	1	1	1	1	1
2	0.131	0.205	0.371	0.769	1	1	1	1
3	0.099	0.154	0.260	0.487	1	1	1	1
4	0.084	0.131	0.214	0.378	0.732	1	1	1
5	0.075	0.117	0.189	0.324	0.592	0.816	1	1
6	0.069	0.108	0.173	0.291	0.511	0.701	0.983	1
8	0.062	0.097	0.154	0.255	0.426	0.578	0.782	0.956
10	0.057	0.091	0.143	0.234	0.383	0.517	0.678	0.836
12	0.055	0.086	0.136	0.221	0.357	0.482	0.619	0.766
14	0.052	0.083	0.131	0.212	0.340	0.459	0.582	0.721
20	0.049	0.078	0.121	0.196	0.311	0.423	0.524	0.655
30	0.046	0.074	0.114	0.184	0.290	0.397	0.487	0.614
40	0.044	0.071	0.111	0.178	0.280	0.385	0.471	0.596
50	0.043	0.070	0.109	0.174	0.274	0.378	0.461	0.586

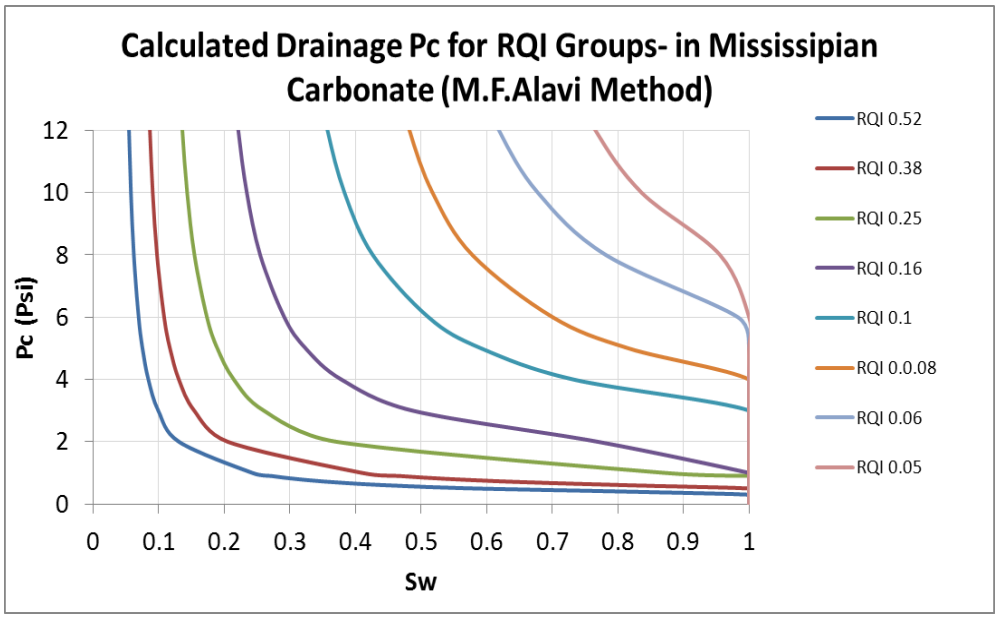

Figure 14: Calculated drainage Pc curve for the Mississippian carbonate

Base on the above procedure, assuming free water level at 3,766 ft and oil water density of 0.83 and 1.11 g/cm3 respectively, initial water saturation of Well 1-32 was calculated using equations 22 and 23. The calculated initial water saturation is shown and compared with the NMR water saturation in fig. A25 (Appendix A). There is a small discrepancy between the two saturations.

g. Calculation of Imbibition Capillary Pressure Curves

Normalized non-wetting phase water saturation is defined according to equation 26 for imbibition.

$$S_{nwn} = \frac{1-S_{wi}-S_{or}}{1-S_{wir}-S_{or}} \qquad \text{(Equation 26)}$$

Snwn is equal to 0 when Pc is 0; therefore, EQR in terms of entry pressure and Pc should be expressed by the following equation:

$$EQR = \frac{P_e}{P_c+P_e} \qquad \text{(Equation 27)}$$

In previous paragraphs, equation 14 was proposed for derivation of initial water saturation for imbibition cases in terms of Swir, Sor, and Snwn. Correlations for Swir, Sor, and Snwn were proposed. Substituting these correlations in equation 14 result in two equations that give initial water saturation based on RQI and Pc: the first (equation 28) is for the chat conglomerate and the second (equation 29) was derived for the carbonate section of the Mississippian formation.

$$S_{wi} = 0.427RQI^{-0.407} - \left(1 - 0.00155\frac{0.1616RQI^{-1.761}}{P_c+0.1616RQI^{-1.761}}\right)\left(1 - \left(\frac{0.1616RQI^{-1.761}}{P_c+0.1616RQI^{-1.761}}\right)^{0.569}\right)(-12.885RQI^2 + 8.031RQI - 1.4924 + 0.427RQI^{-0.407}) \qquad \text{(Equation 28)}$$

$$S_{wi} = 0.5811RQI^{-0.139} - \left(1 - 0.5245\frac{0.1467RQI^{-1.312}}{P_c+0.1467RQI^{-1.312}}\right)\left(1 - \left(\frac{0.1467RQI^{-1.312}}{P_c+0.1467RQI^{-1.312}}\right)^{3.125}\right)(-0.0202RQI^{-1.127} + 0.5811RQI^{-0.139})$$

(Equation29)

Based on equation 28 for imbibition, eight capillary pressure curves were generated for the chat conglomerate (table 6 and fig. 15).

Table 6: Imbibition Pc table for different RQI groups in the Mississippian chat

a 0.001553	b 0.570	Imbibition Table in Mississippian Chat						
RQI	0.32	0.28	0.245	0.22	0.2	0.175	0.145	0.12
Pe	1.20	1.52	1.92	2.33	2.75	3.48	4.84	6.76
Sor	0.32	0.3	0.27	0.24	0.21	0.155	0.09	0.03
Swir	0.23	0.26	0.3	0.34	0.4	0.48	0.58	0.7
Pc	**Swi**							
0	0.679	0.700	0.730	0.760	0.790	0.845	0.910	0.970
0.1	0.659	0.684	0.718	0.750	0.782	0.839	0.906	0.968
0.2	0.642	0.670	0.706	0.741	0.775	0.834	0.902	0.966
0.3	0.626	0.657	0.696	0.732	0.768	0.828	0.899	0.963
0.4	0.612	0.645	0.686	0.724	0.761	0.823	0.895	0.961
0.5	0.599	0.634	0.677	0.716	0.755	0.818	0.892	0.959
0.6	0.587	0.624	0.668	0.709	0.749	0.813	0.889	0.957
0.7	0.576	0.615	0.660	0.702	0.743	0.809	0.886	0.955
0.8	0.566	0.606	0.653	0.695	0.737	0.804	0.883	0.953
0.9	0.557	0.598	0.646	0.689	0.732	0.800	0.880	0.951
1	0.548	0.590	0.639	0.683	0.727	0.796	0.877	0.950
2	0.487	0.533	0.587	0.635	0.686	0.762	0.851	0.933
3	0.450	0.497	0.552	0.602	0.656	0.736	0.831	0.919
4	0.425	0.471	0.527	0.578	0.634	0.716	0.814	0.907
5	0.406	0.452	0.507	0.559	0.616	0.700	0.800	0.897
6	0.392	0.437	0.492	0.543	0.602	0.686	0.789	0.888
8	0.371	0.415	0.469	0.520	0.579	0.665	0.769	0.873
10	0.356	0.399	0.452	0.502	0.563	0.649	0.754	0.861
12	0.345	0.387	0.439	0.489	0.550	0.636	0.742	0.851
14	0.336	0.377	0.429	0.478	0.539	0.626	0.732	0.843
20	0.318	0.357	0.408	0.456	0.517	0.603	0.710	0.823
30	0.300	0.338	0.387	0.434	0.495	0.581	0.687	0.803
40	0.290	0.327	0.374	0.420	0.482	0.567	0.673	0.790
50	0.283	0.319	0.366	0.411	0.472	0.557	0.663	0.780

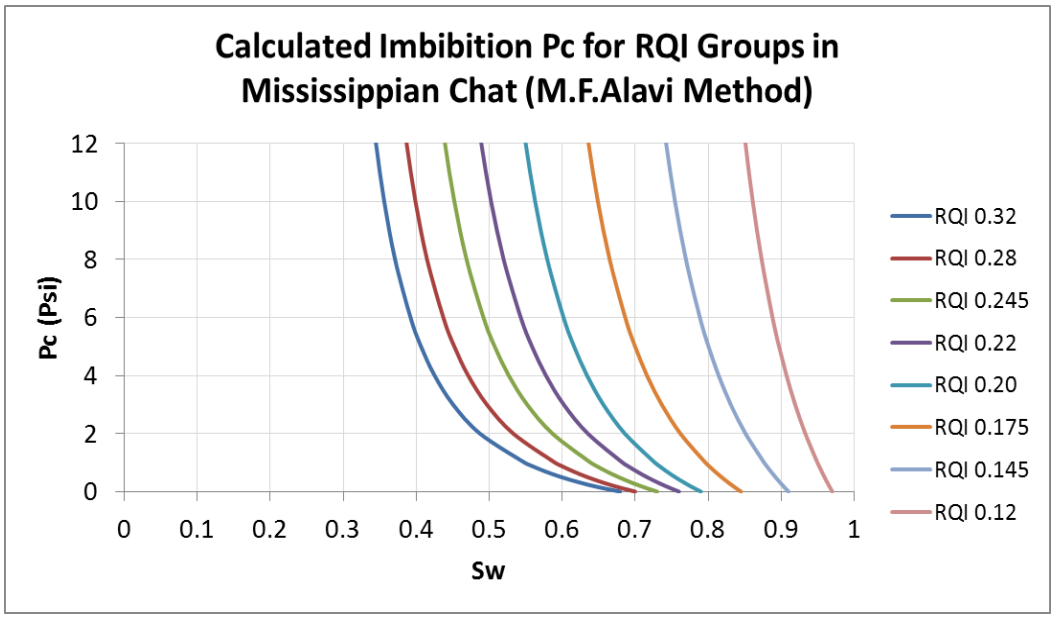

Figure 15: Calculated imbibition Pc curve for the Mississippian chat

For the carbonate section, equation 27 was used to calculate eight capillary pressure curves (table 7 and fig. 16).

Table 7: Imbibition Pc table for different RQI groups in the Mississippian carbonate

a 0.52	b 3.12	Imbibition Table in Mississippian Carbonate						
RQI	0.52	0.38	0.25	0.16	0.1	0.08	0.06	0.05
Pe	0.35	0.52	0.90	1.62	3.01	4.03	5.88	7.47
Sor	0.36	0.34	0.31	0.28	0.25	0.22	0.20	0.17
Swir	0.04	0.065	0.1	0.16	0.25	0.35	0.425	0.55
Pc	**Swi**							
0	0.636	0.658	0.685	0.722	0.750	0.780	0.800	0.826
0.1	0.443	0.518	0.599	0.673	0.726	0.765	0.791	0.820
0.2	0.334	0.423	0.530	0.631	0.703	0.750	0.782	0.815
0.3	0.268	0.358	0.475	0.593	0.683	0.736	0.773	0.810
0.4	0.226	0.311	0.431	0.560	0.663	0.723	0.765	0.805
0.5	0.197	0.277	0.396	0.531	0.645	0.710	0.757	0.800
0.6	0.175	0.251	0.366	0.505	0.628	0.698	0.749	0.795
0.7	0.159	0.230	0.342	0.482	0.612	0.687	0.741	0.791
0.8	0.146	0.214	0.321	0.462	0.597	0.676	0.734	0.786
0.9	0.136	0.200	0.304	0.443	0.583	0.665	0.727	0.782
1	0.128	0.189	0.289	0.427	0.570	0.656	0.720	0.777
2	0.088	0.133	0.208	0.327	0.477	0.580	0.663	0.741
3	0.073	0.112	0.176	0.281	0.424	0.532	0.623	0.713
4	0.065	0.102	0.159	0.255	0.390	0.500	0.593	0.692
5	0.060	0.095	0.149	0.238	0.367	0.477	0.571	0.675
6	0.057	0.090	0.141	0.227	0.351	0.460	0.553	0.661
8	0.053	0.084	0.132	0.212	0.329	0.437	0.528	0.641
10	0.050	0.080	0.126	0.202	0.315	0.422	0.511	0.627
12	0.049	0.078	0.122	0.196	0.305	0.412	0.499	0.616
14	0.048	0.076	0.119	0.191	0.298	0.404	0.490	0.609
20	0.045	0.073	0.113	0.182	0.285	0.389	0.473	0.593
30	0.044	0.070	0.109	0.175	0.274	0.377	0.458	0.580
40	0.043	0.069	0.107	0.172	0.268	0.371	0.451	0.574
50	0.042	0.068	0.105	0.169	0.265	0.367	0.446	0.569

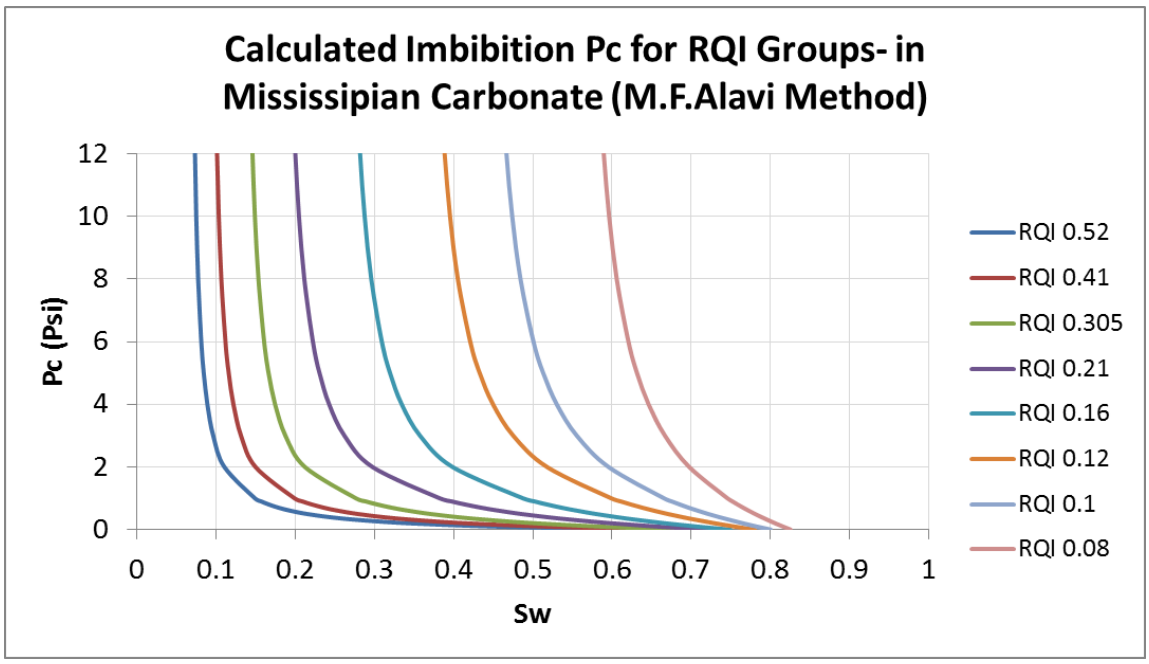

Figure 16: Calculated imbibition Pc curve for the Mississippian carbonate

h. Application of Pc Curves in Modelling

The Mississippian reservoir at present lacks SCAL data with Pc curves. These Pc curves are produced using NMR data, generalized data published in the literature, and correlations derived from data of other carbonate and sandstone reservoirs. They could be calibrated against lab Pc curves when such data become available. In the absence of lab data, modelling could be initiated with the proposed curves.

The model should have two main zones or layers: the chat conglomerate and the carbonate section. The main layers should be divided into six zones. Porosity and permeability should be populated into the gridding by the right algorithm within subzones, which have been shown in the well layouts. The RQI should be calculated for each grid cell. Based on the RQI of the cells, eight saturation regions should be defined in the chat conglomerate corresponding to the RQI ranges of Pc curves. Also eight saturation regions should be defined in the carbonate section of the reservoir. The RQI of the regions should correspond to the RQI of the proposed PC curves.

IV- Imbibition Relative Permeability Curves

Relative permeability tables are critical data in reservoir simulation. It was proposed before to define eight saturation regions in the chat conglomerate model and eight in the carbonate section, based on the RQI of grid cells. Assuming that the reservoir is under saturated and that its pressure will always remain above bubble point pressure, only oil and water relative permeability tables are estimated for eight saturation regions each in the chat conglomerate and carbonate section of the Mississippian reservoir. To estimate relative permeability for these regions, the following modified Corey equations were used.

$$Kro = kro_{Swi}(1 - Sw_D)^p \quad \text{(Equation 30)}$$

$$Krw = krw_{Sorw} * (Sw_D)^q \quad \text{(Equation 31)}$$

$$Sw_D = \frac{(Sw - Swc)}{(1 - Sorw - Swc)} \quad \text{(Equation 32)}$$

Corey exponent *p* (Oil Corey Exponent) and *q* (Water Corey Exponent) were assumed at 2.5 and 1.5, respectively, based on experience from SCAL in other fields. Critical water saturation (Swc) was taken from Pc curves where capillary pressure is 10 psi. Residual oil saturation (Sor) was previously estimated by equations 19 and 20 based on SCAL data of several fields.

Oil relative permeability at Swc and max water permeability at Sor was derived from equations 33 and 34, which are correlations obtained from SCAL data in other fields.

$$Krw_{Sorw} = 0.1371 RQI^{-0.348} \quad \text{(Equation 33)}$$

$$Kro_{Swi} = 0.8909 RQI^{0.0194} \quad \text{(Equation 34)}$$

Tables B1 to B8 (Appendix B) present the parameters that were used to calculate the relative permeability of the chat conglomerate. Tables C1 to C8 (Appendix C) present the same parameters for the carbonate section of the Mississippian reservoir.

Eight sets of relative permeability tables were generated for the chat conglomerate (fig. 17), and eight sets of these curves were calculated for the carbonate section (fig. 18). All eight relative permeability curves for each chat and carbonate section can be found in Appendix B (figs. B1 to B8) and Appendix C (figs. C1 to C8).

Tables 8 and 9 and figs. 19 and 20 present the relative permeability for the first RQI group of the chat and carbonate sections, respectively.

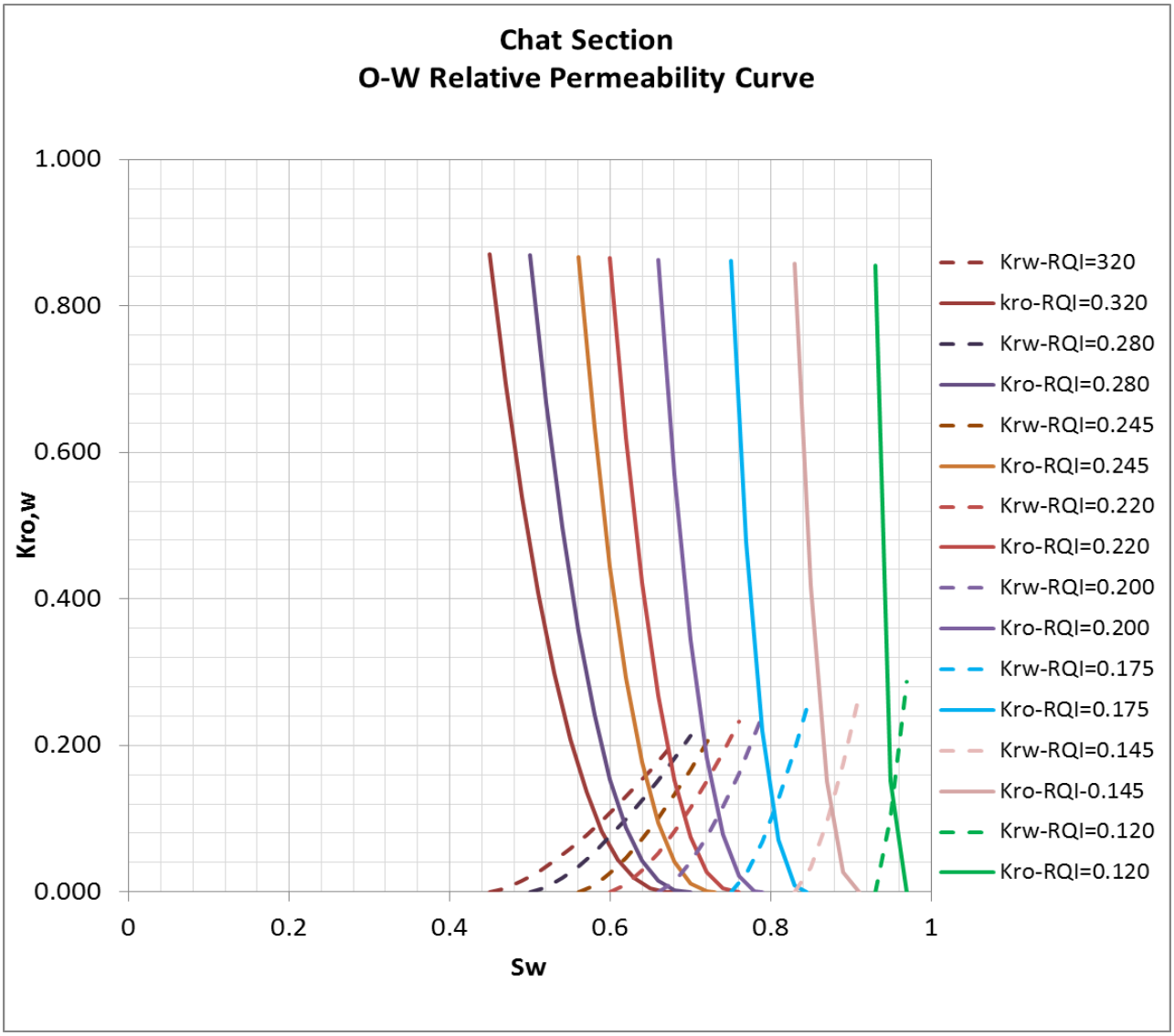

Figure 17: Relative permeability curves for the chat section at different RQI groups

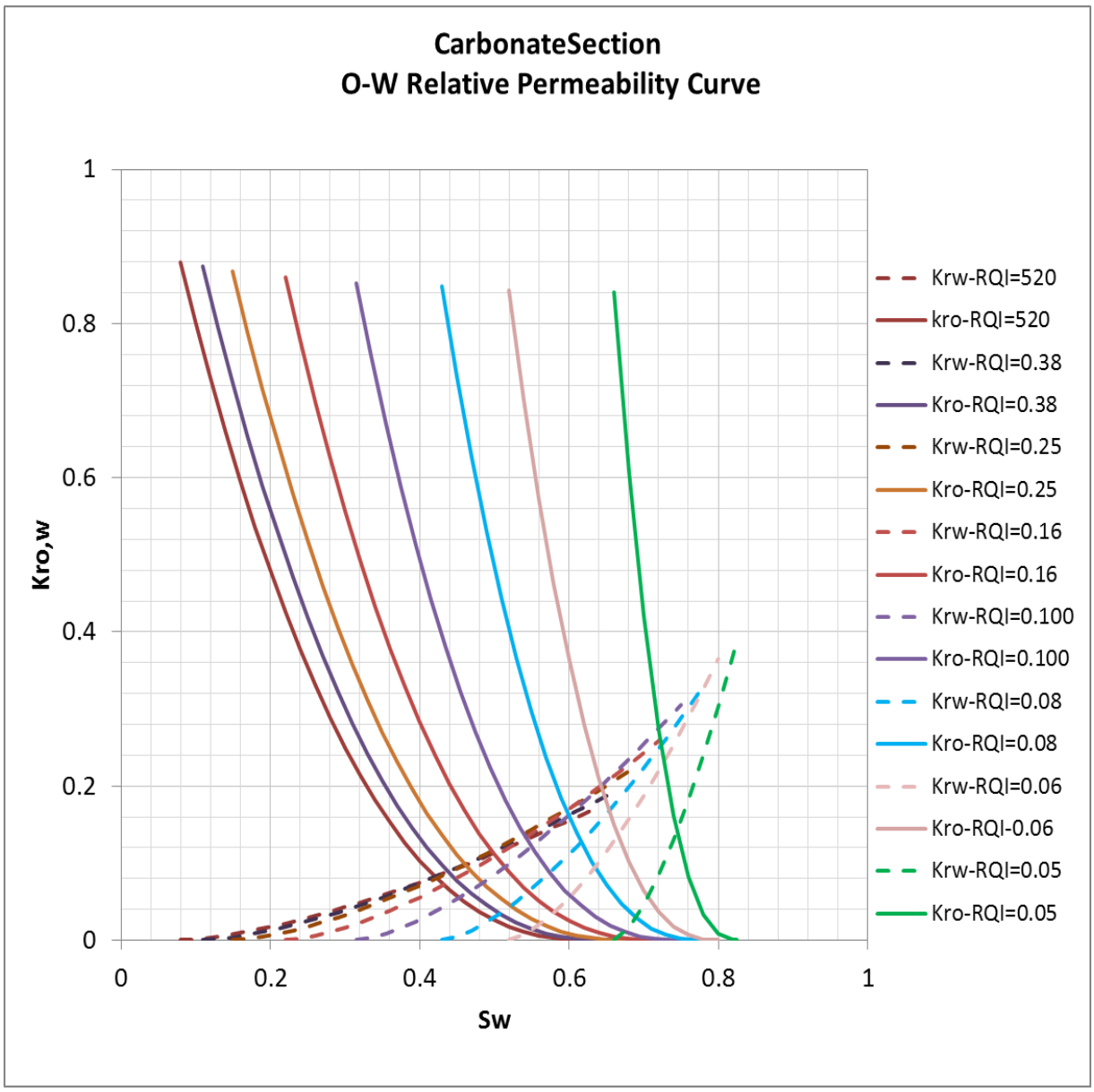

Figure 18: Relative permeability curves for the carbonate section at different RQI groups

Table 8: Relative permeability data for the chat section at RQI= 0.320

RQI=			0.320	
Sor	Swc	Chat	Krw max	Kro max
0.321	0.45	1	0.204	0.871
q	1.5		p	2.5
Sw	So	SwD	Krw	kro
0.450	0.550	0.000	0.000	0.871
0.470	0.530	0.087	0.005	0.694
0.490	0.510	0.174	0.015	0.540
0.510	0.490	0.262	0.027	0.408
0.530	0.470	0.349	0.042	0.298
0.550	0.450	0.436	0.059	0.208
0.570	0.430	0.523	0.077	0.137
0.590	0.410	0.610	0.097	0.083
0.610	0.390	0.698	0.119	0.044
0.630	0.370	0.785	0.142	0.019
0.650	0.350	0.872	0.166	0.005
0.670	0.330	0.959	0.191	0.000
0.679	0.321	1.000	0.204	0.000

Table 9: Relative permeability data for the carbonate section at RQI=0.520

RQI=			0.520	
Sor	Swc	Carbonate	Krw max	Kro max
0.364	0.08	1	0.172	0.880
q	1.5		p	2.5
Sw	So	SwD	Krw	kro
0.080	0.920	0.000	0	0.880
0.100	0.900	0.036	0.001173	0.803
0.120	0.880	0.072	0.003318	0.730
0.140	0.860	0.108	0.006096	0.661
0.160	0.840	0.144	0.009385	0.597
0.180	0.820	0.180	0.013116	0.536
0.200	0.800	0.216	0.017241	0.479
0.220	0.780	0.252	0.021726	0.426
0.240	0.760	0.288	0.026544	0.377
0.260	0.740	0.324	0.031674	0.331
0.280	0.720	0.359	0.037097	0.289
0.300	0.700	0.395	0.042798	0.250
0.320	0.680	0.431	0.048765	0.215
0.340	0.660	0.467	0.055	0.182
0.360	0.640	0.503	0.061	0.153
0.380	0.620	0.539	0.068	0.127
0.400	0.600	0.575	0.075	0.104
0.420	0.580	0.611	0.082	0.083
0.440	0.560	0.647	0.090	0.065
0.460	0.540	0.683	0.097	0.050
0.480	0.520	0.72	0.105	0.037
0.500	0.500	0.755	0.113	0.026
0.520	0.480	0.791	0.121	0.018
0.540	0.460	0.827	0.129	0.011
0.560	0.440	0.863	0.138	0.006
0.580	0.420	0.899	0.147	0.003
0.600	0.400	0.935	0.156	0.001
0.620	0.380	0.971	0.165	0.0001
0.636	0.364	1.000	0.172	0.000

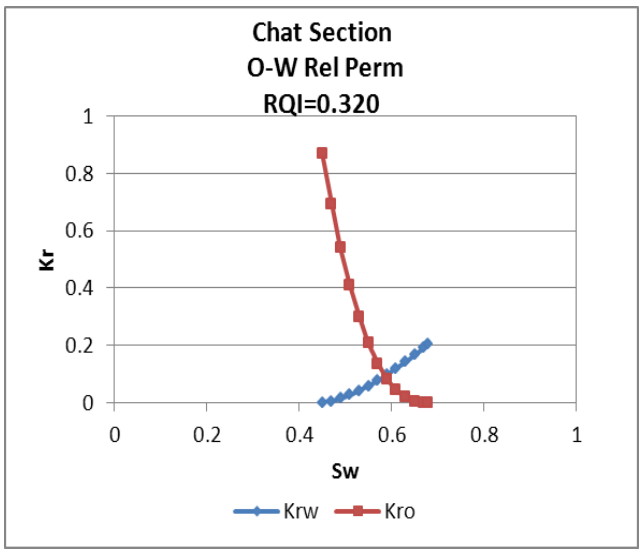

Figure 19: Relative permeability curve for the chat section at RQI= 0.320

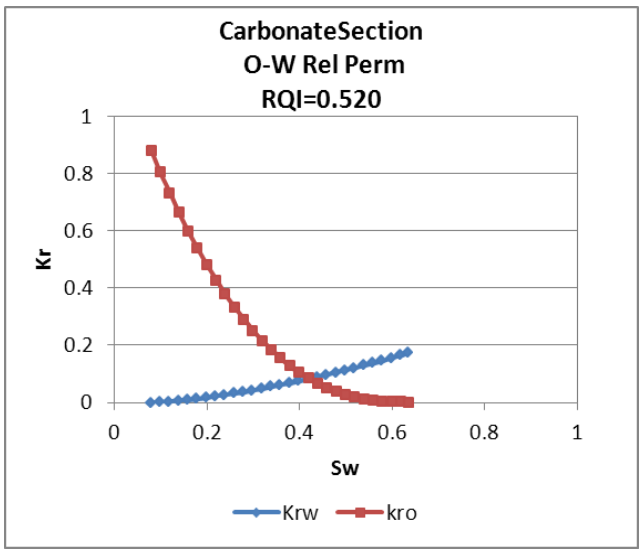

Figure 20: Relative permeability curve for the carbonate section at RQI= 0.520

V- Reservoir Model Construction and Uncertainties

The reservoir model can be constructed using the data that are presented in this report. However, some of the data, as will be discussed below, might not be accurate and may make history matching of the reservoir dynamic model difficult. Data uncertainties, utilization of the data during modeling, and improvement of model properties during modeling and history matching of model results are addressed here.

a. Porosity

Calculated porosity in old wells is from old neutron logs that have been normalized. The accuracy of these porosities and the porosity of wells with poor log quality is suspect. It is suggested to divide wells into three groups based on reliability of porosity: A) good, B) fair, and C) poor.

During modeling, if poor wells do not follow the trend of porosity of good wells or they do not conform to geological information about porosity trends in the field, they could be omitted from the data set for porosity modeling. In the same manner, fair wells can be verified for accuracy and they could be removed from the data set.

After construction of the model, original oil in-place (OOIP)can be calculated by the model and compared with OOIP from material balance calculation. If a big discrepancy is observed, the porosity of poor and fair wells can be adjusted by a factor within the limits of the good wells. Then the model should be modified based on adjusted porosities.

During history matching, there may be a mismatch between the actual production data during the early production period when water cut is negligible and production from the dynamic model. In these cases, if the well is a poor or a fair well, the porosity should be suspected because permeability is a function of porosity. Necessary adjustments of porosity within limits dictated by the good wells may be done and, consequently, permeability can be recalculated based on adjusted porosity.

b. Permeability

FZI was not assigned to wells in a theoretically correct way. Therefore, there is uncertainty in the permeability of wells with the exceptions of Well 1-32 and Peasel 1 well. Early production history of the wells can be used to tune permeability of the wells. If there is a mismatch between early production from the dynamic model and actual production of the wells, permeability of the well can be adjusted by a factor and the model can be revised.

In this report, regression was not used to assign FZI from Well 1-32 to other wells. A correlation between FZI and log signatures could be found in Well 1-32 and applied to other wells that have similar well logs. This procedure could be applied to wells having good neutron, density, GR, shallow, and deep resistivity logs and may provide a better permeability model for simulation.

c. Capillary Pressure

SCAL data were not available for this reservoir. Therefore, Pc curves were generated based on end point from the NMR of Well 1-32 and by adapting the shape of generalized Pc curves published in literature for this formation. Naturally, when SCAL data become available, Pc curves could be adjusted.

d. Relative Permeability

The proposed relative permeability curves were not derived from actual SCAL data on core samples from this field. When SCAL data of the cores of the field arrive, end points and Corey exponents of the curves will be adjusted.

Moreover, late production history of the wells when there is water production will be used during history matching to modify the relative permeability of the rock types.

References

Bhattacharya, S., Byrnes, A. P., and Gerlach, P. M., 2003, Cost-effective integration of geologic and petrophysical characterization with material balance and decline curve analysis to develop a 3D reservoir model for PC-based reservoir simulation to design a waterflood in a mature Mississippian carbonate field with limited log data: Kansas Geological Survey, Open-File Report 2003-31, http://www.kgs.ku.edu/PRS/publication/2003/ofr2003-31/P1-02.html.

Watney, W. L., Guy, W. J., and Byrnes, A. P., 2002, Characterization of Mississippian Osage chat in south-central Kansas: Kansa Geological Survey, Open-File Report 2002-50, http://www.kgs.ku.edu/PRS/Poster/2002/2002-50/P2-06.html.

APPENDIX A.
Techlog layouts

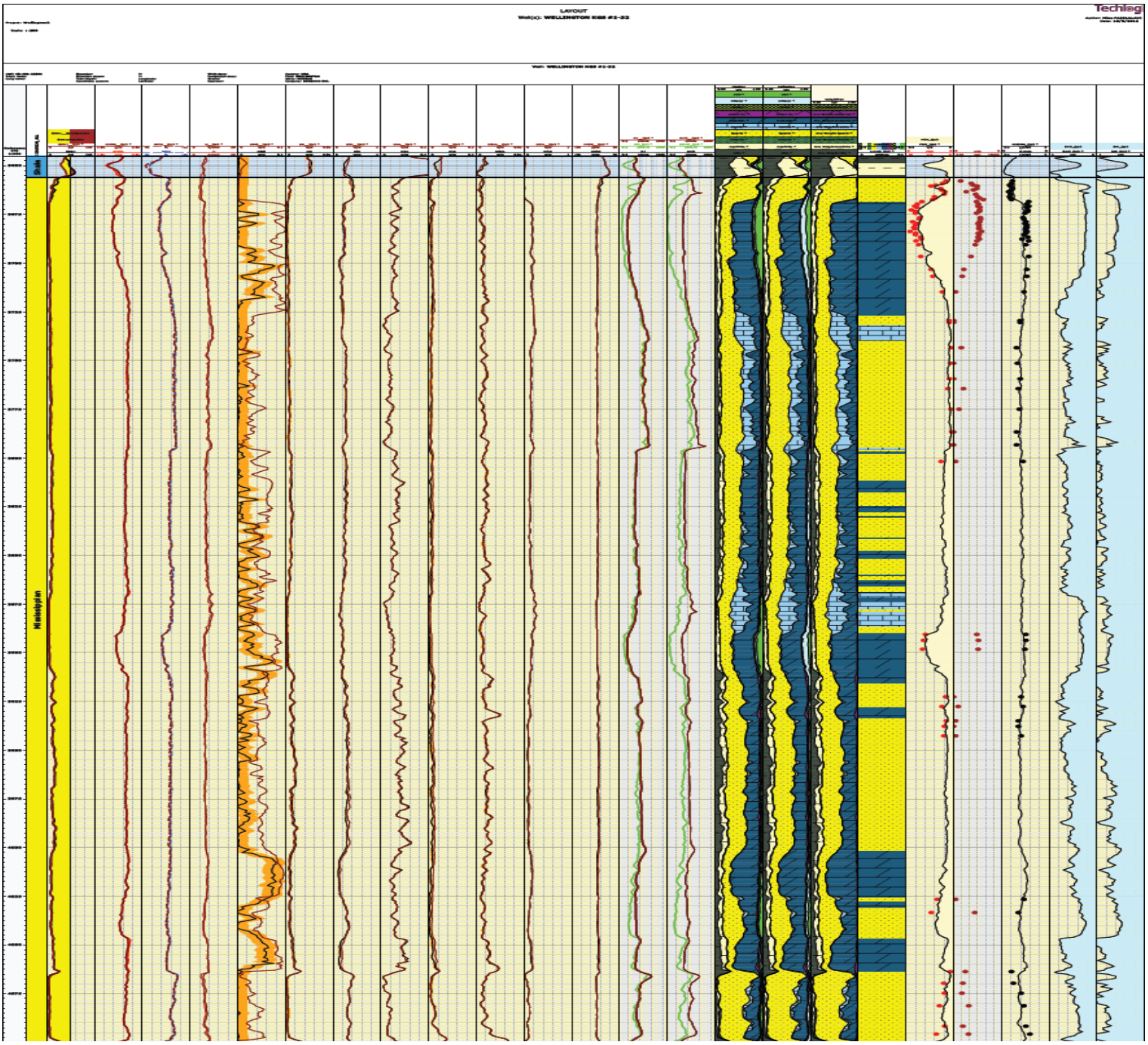

Figure A1: Well 1-32 layout—geochemical and conventional log analyzed by Techlog

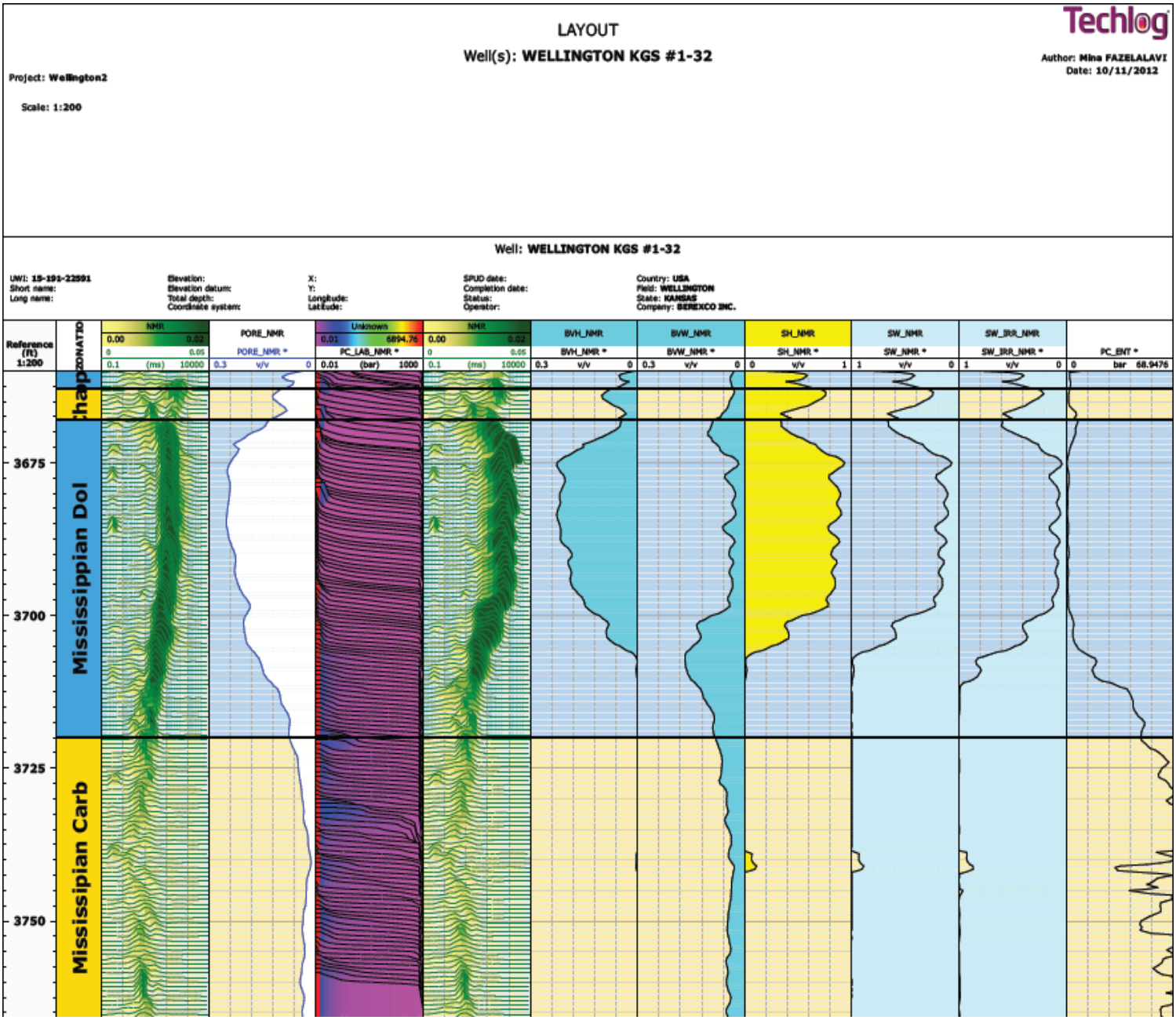

Figure A2: Well 1-32 layout—Porosity, Pc, Swi and Swirr at Pc_irr equal 20 bar

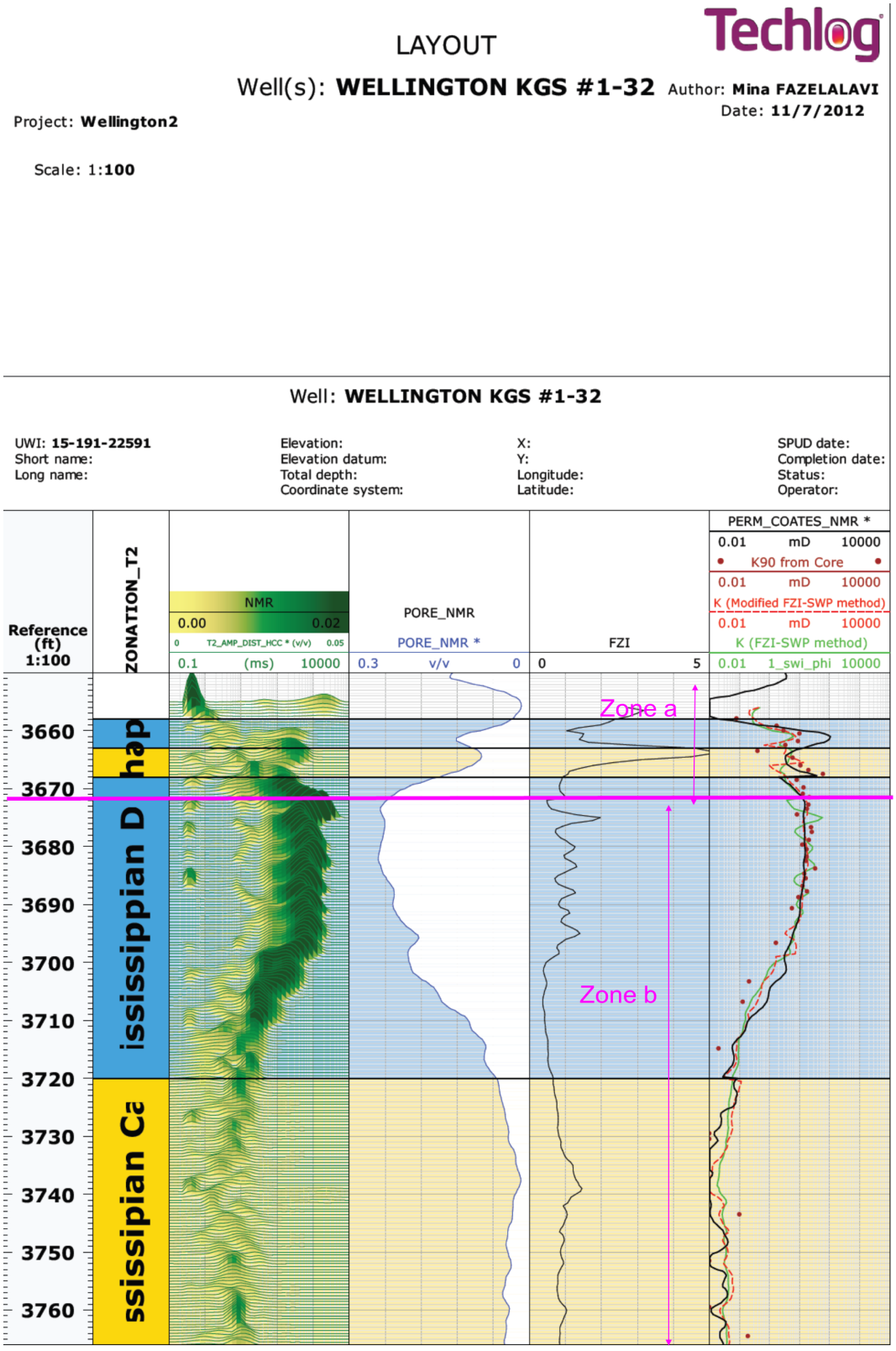

Figure A3: Well 1-32 showing zone a and b. The first column on the right compares Coates permeability and permeability from FZI-SWP with core permeability

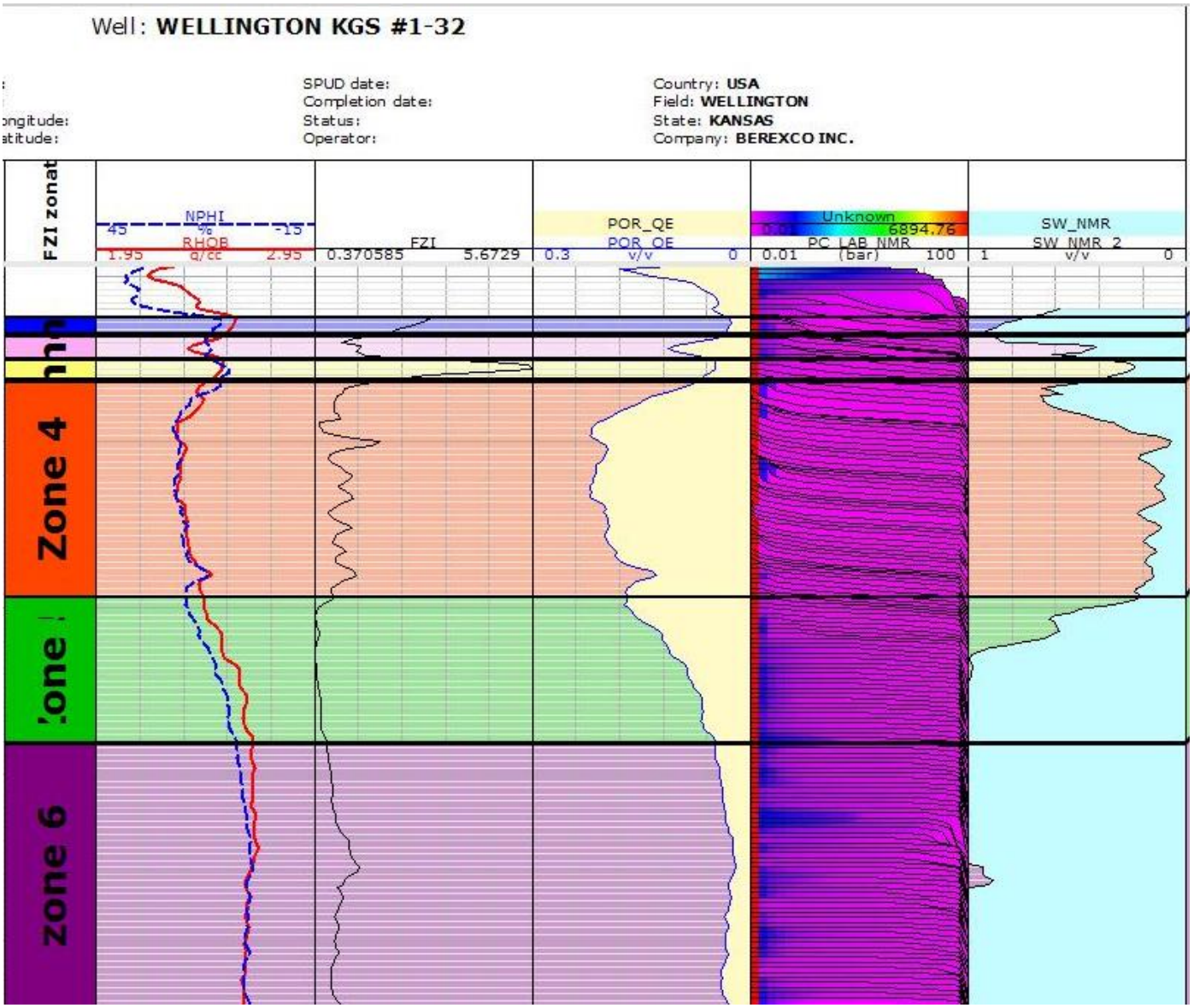

Figure A4: Well 1-32 layout showing six zones based on similar FZI variation in each zone

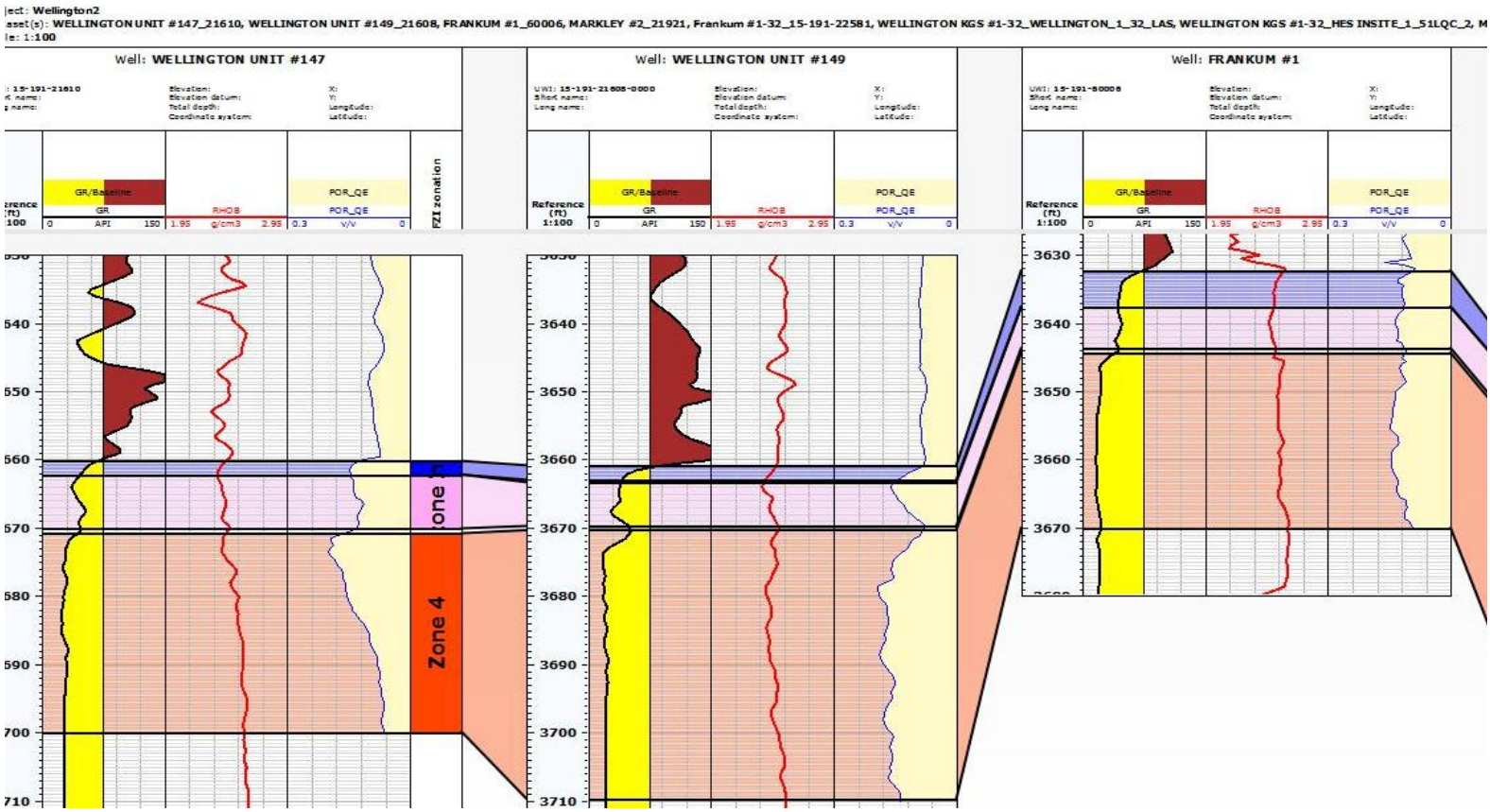

Figure A5: Equivalent zones in wells 147, 149, and Frankum#1 with equal FZI values corresponding to the six zones of Well 1-32

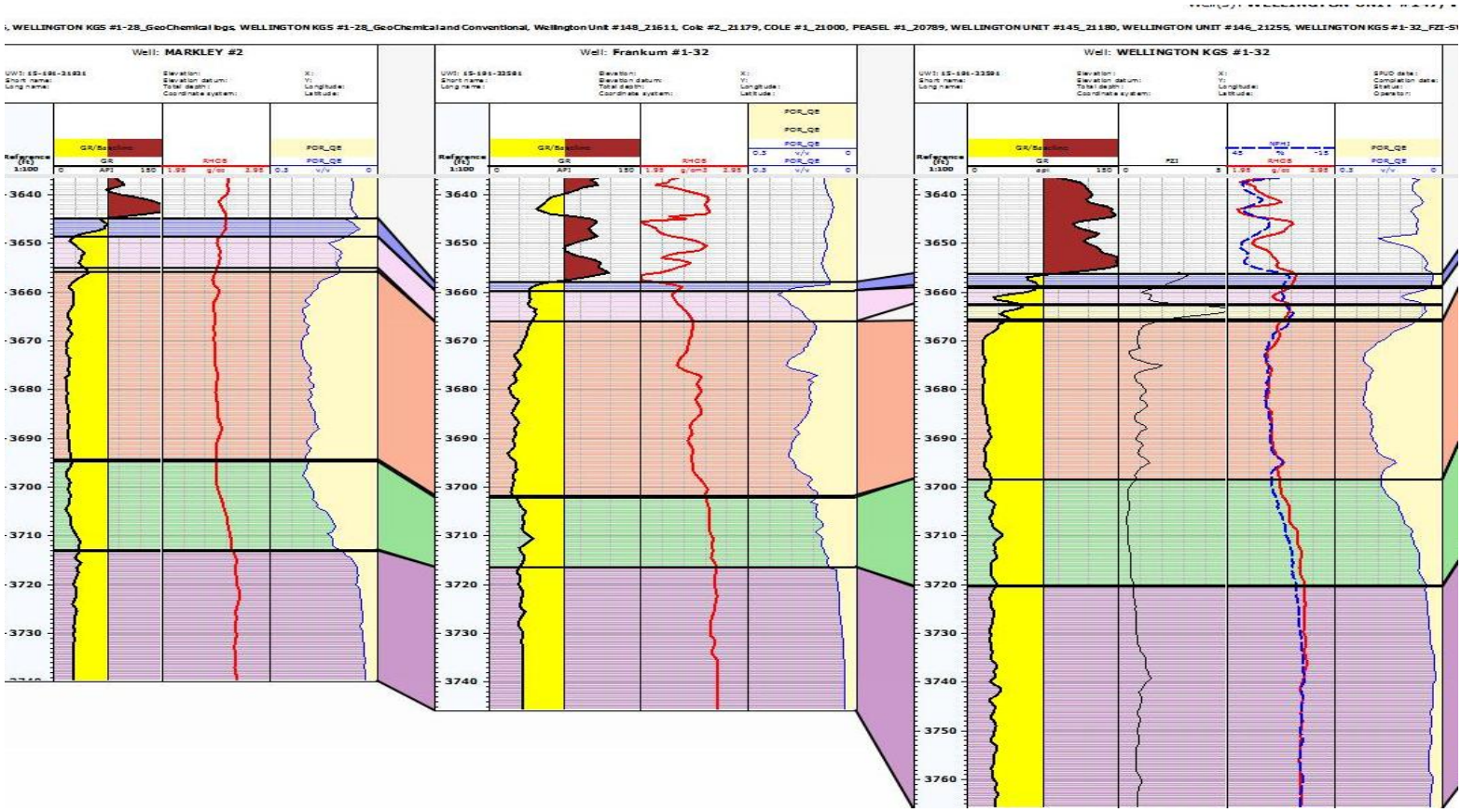

Figure A6: Equivalent zones in wells Markley#2 and Frankum#1-32 with equal FZI values corresponding to the six zones of Well 1-32

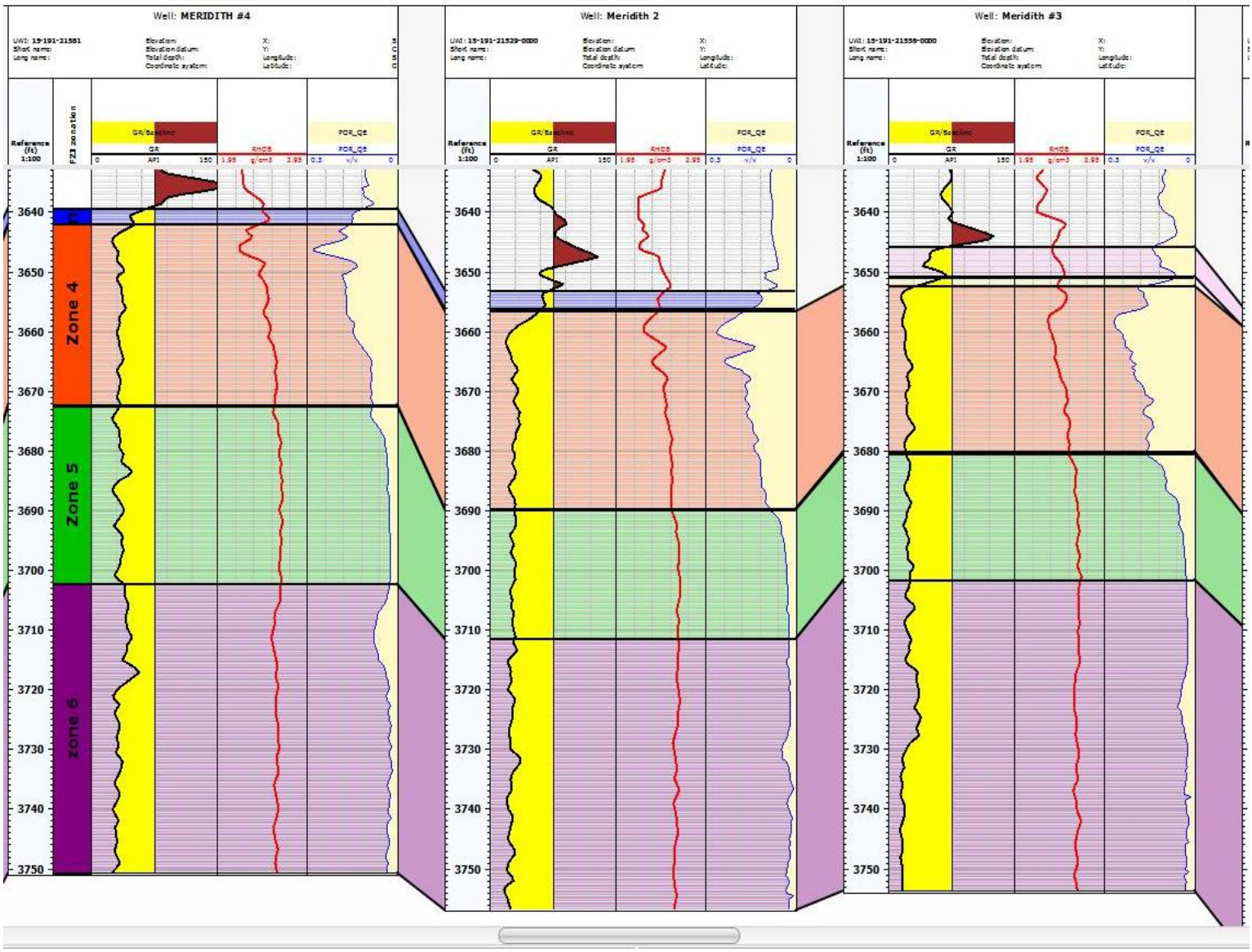

Figure A7: Equivalent zones in wells Meridith#4, Meredith2, and Meridith3 with equal FZI values corresponding to the six zones of Well 1-32

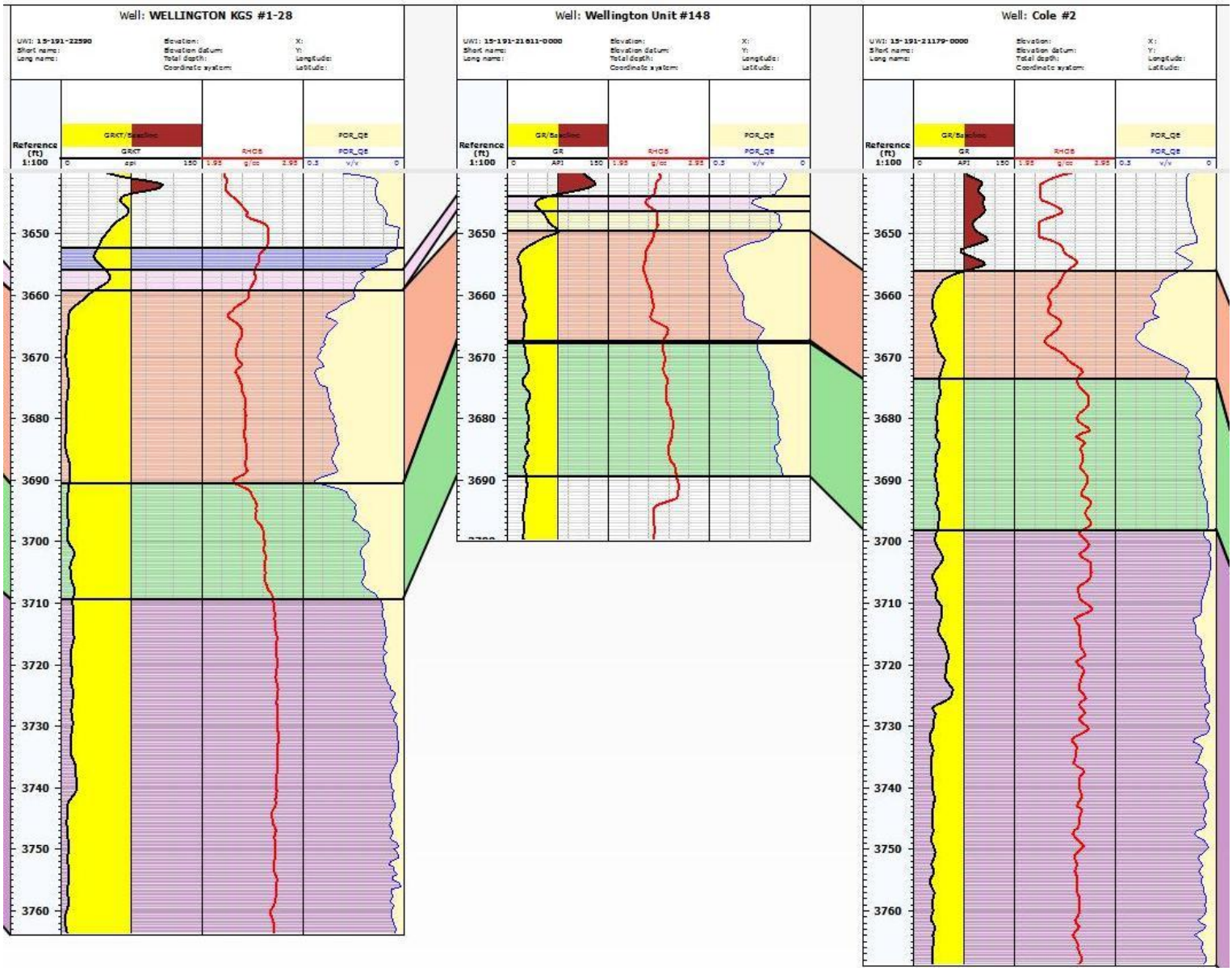

Figure A8: Equivalent zones in wells 1-28, 148, and Cole #2 with equal FZI values corresponding to the six zones of Well 1-32

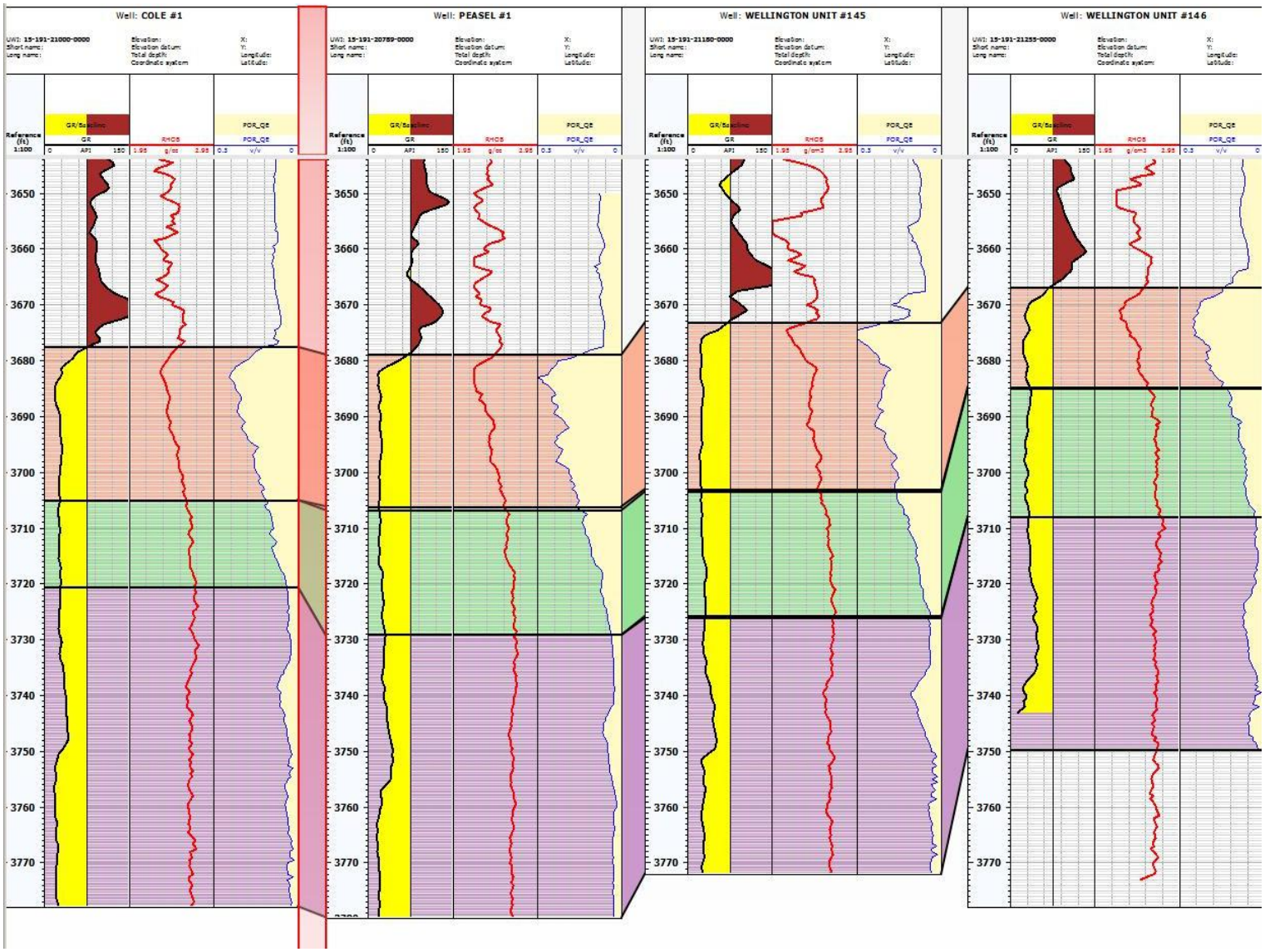

Figure A9: Equivalent zones in wells Cole #1, Peasel #1, 145, and 146 with equal FZI values corresponding to the six zones of Well 1-32

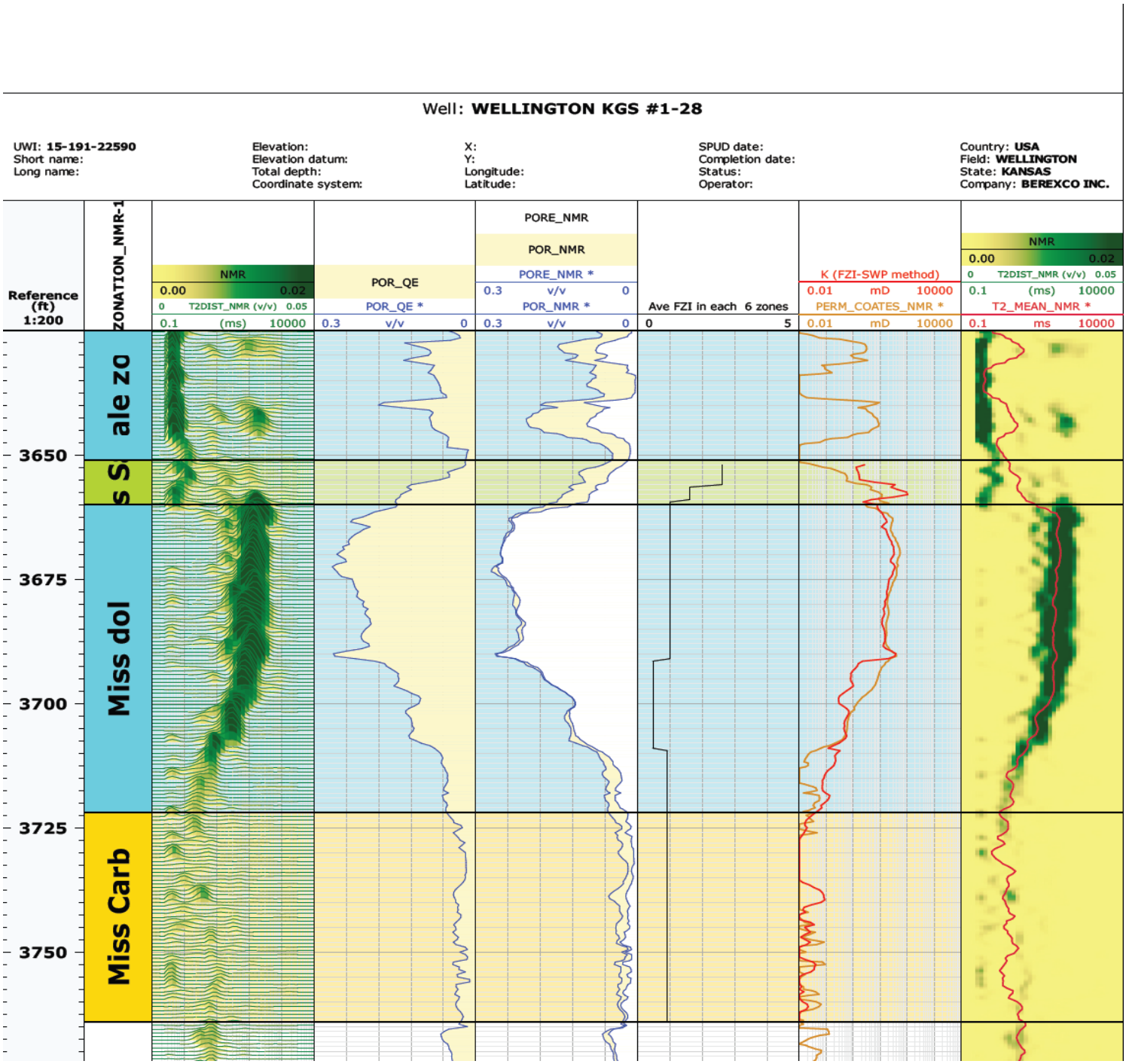

Figure A10: Well 1-28 showing average FZI in each of six zones in track 3 from right and comparing permeability from FZI-SWP method to Coates permeability

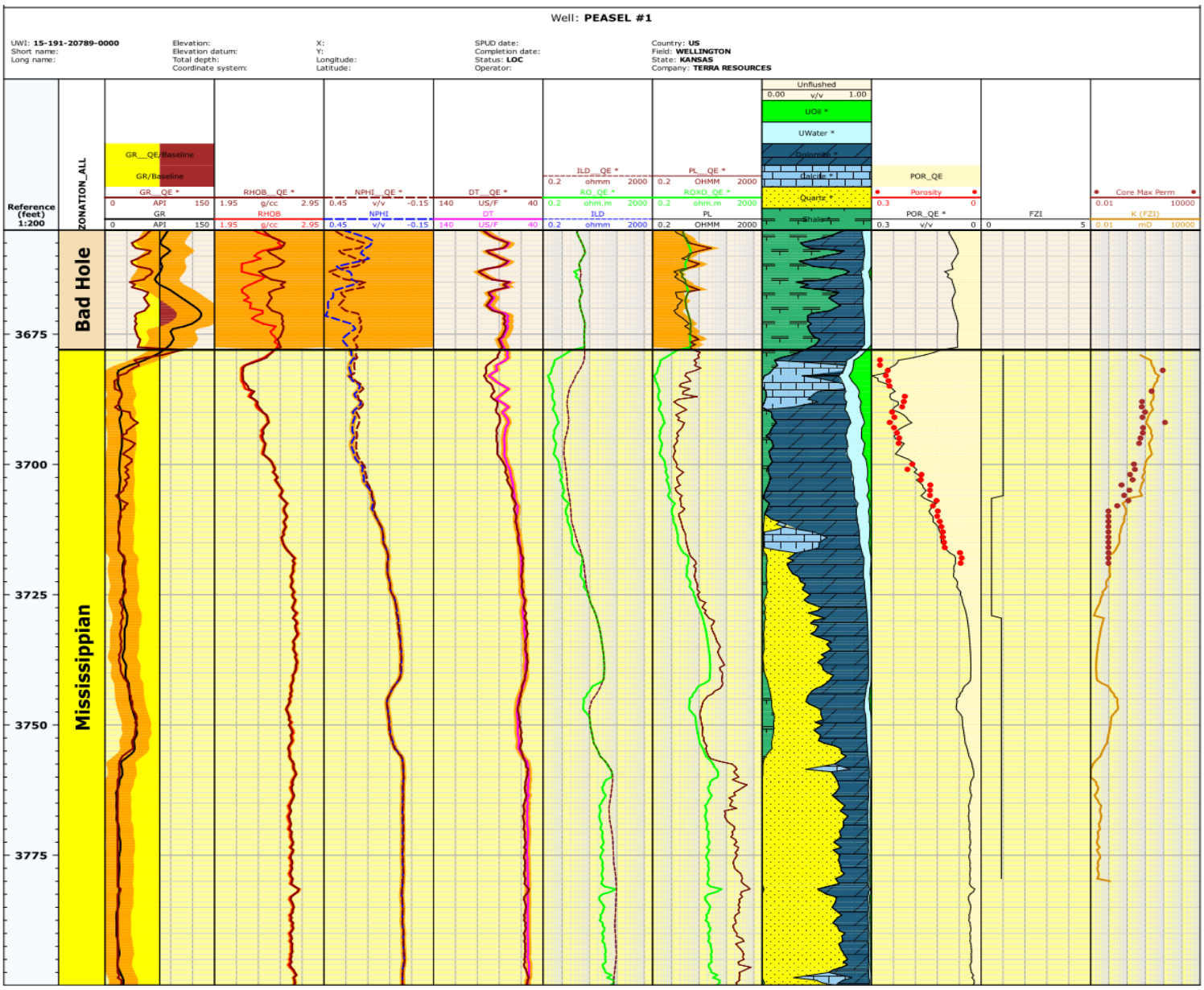

Figure A11: Layout of Peasel #1 comparing permeability from the FZI-SWP method to Coates permeability and showing average FZI in each of the six zones

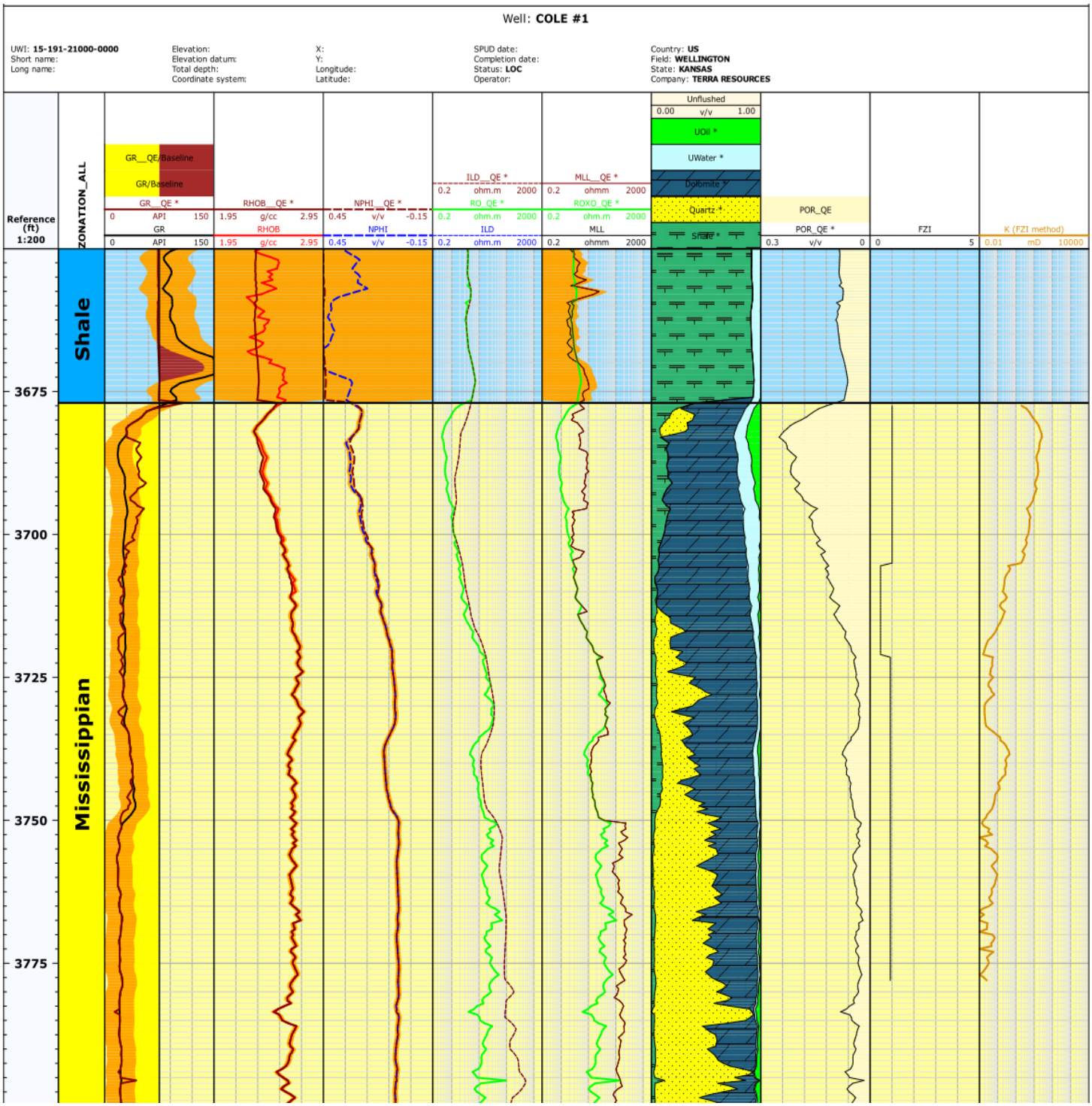

Figure A12: Layout of Cole #1 showing average FZI in each of six zones and permeability from the FZI-SWP method

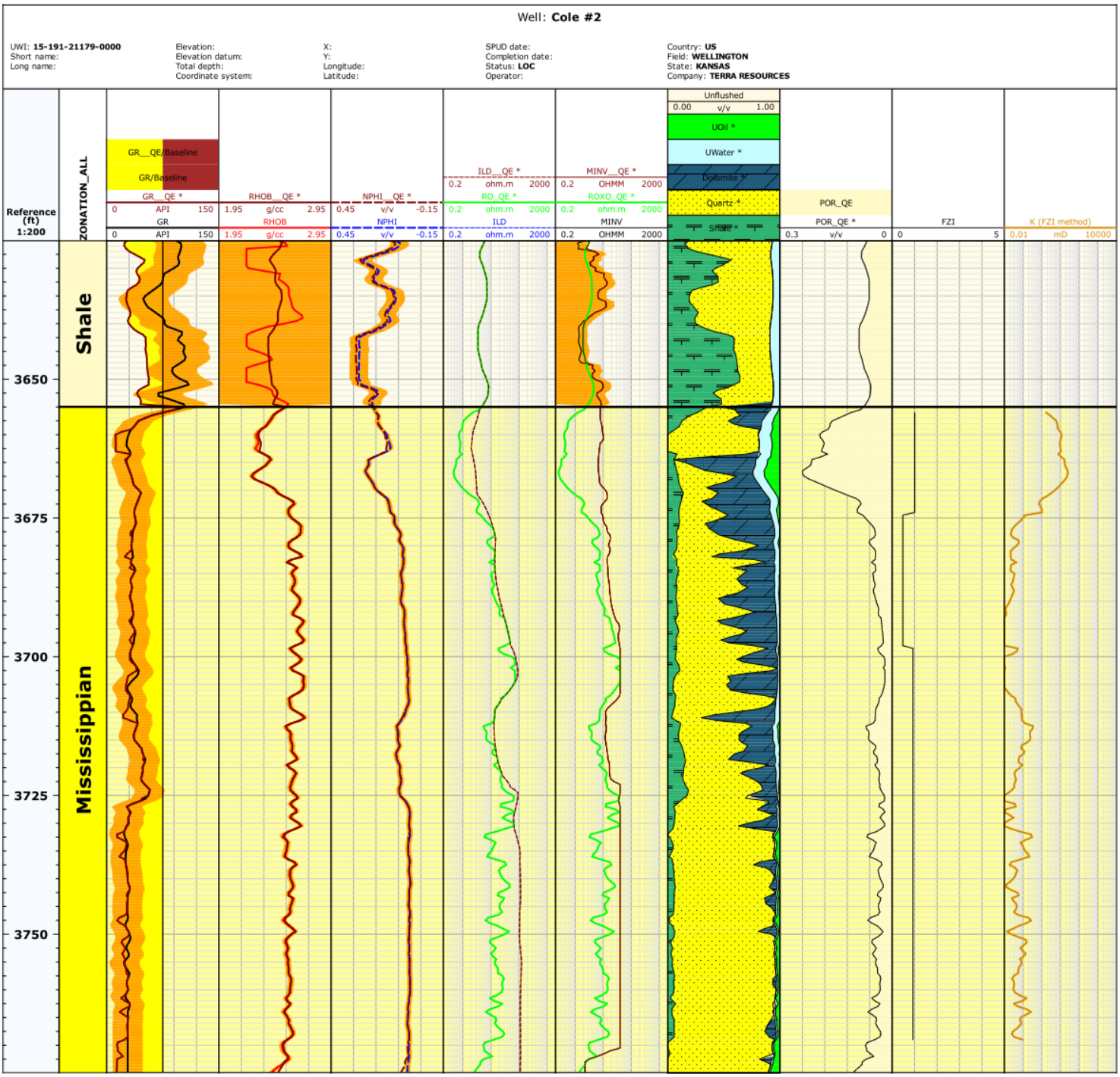

Figure A13: Layout of Cole #2 showing average FZI in each of six zones and permeability from the FZI-SWP method

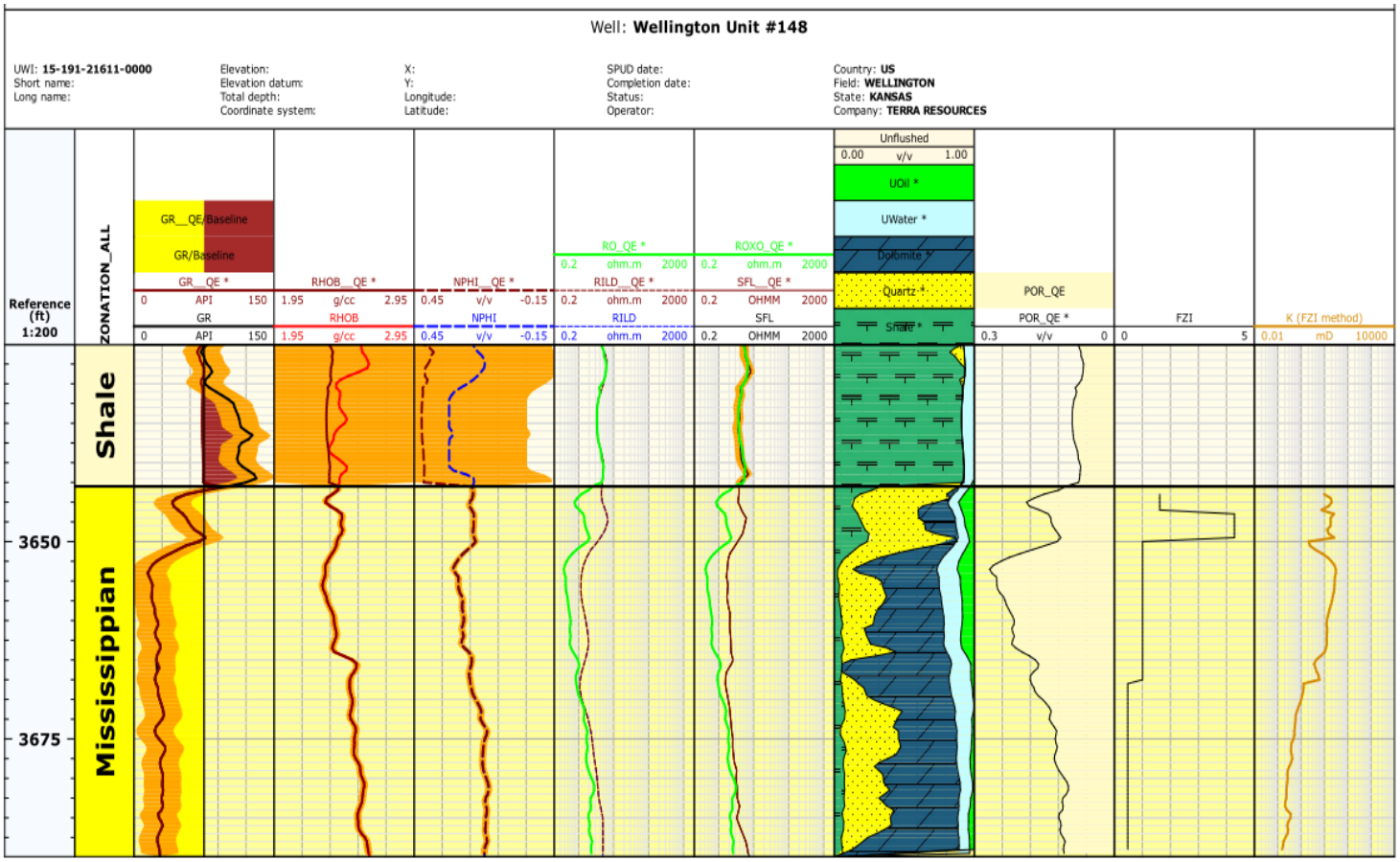

Figure A14: Layout of Well 148 showing average FZI in each of six zones and permeability from the FZI-SWP method

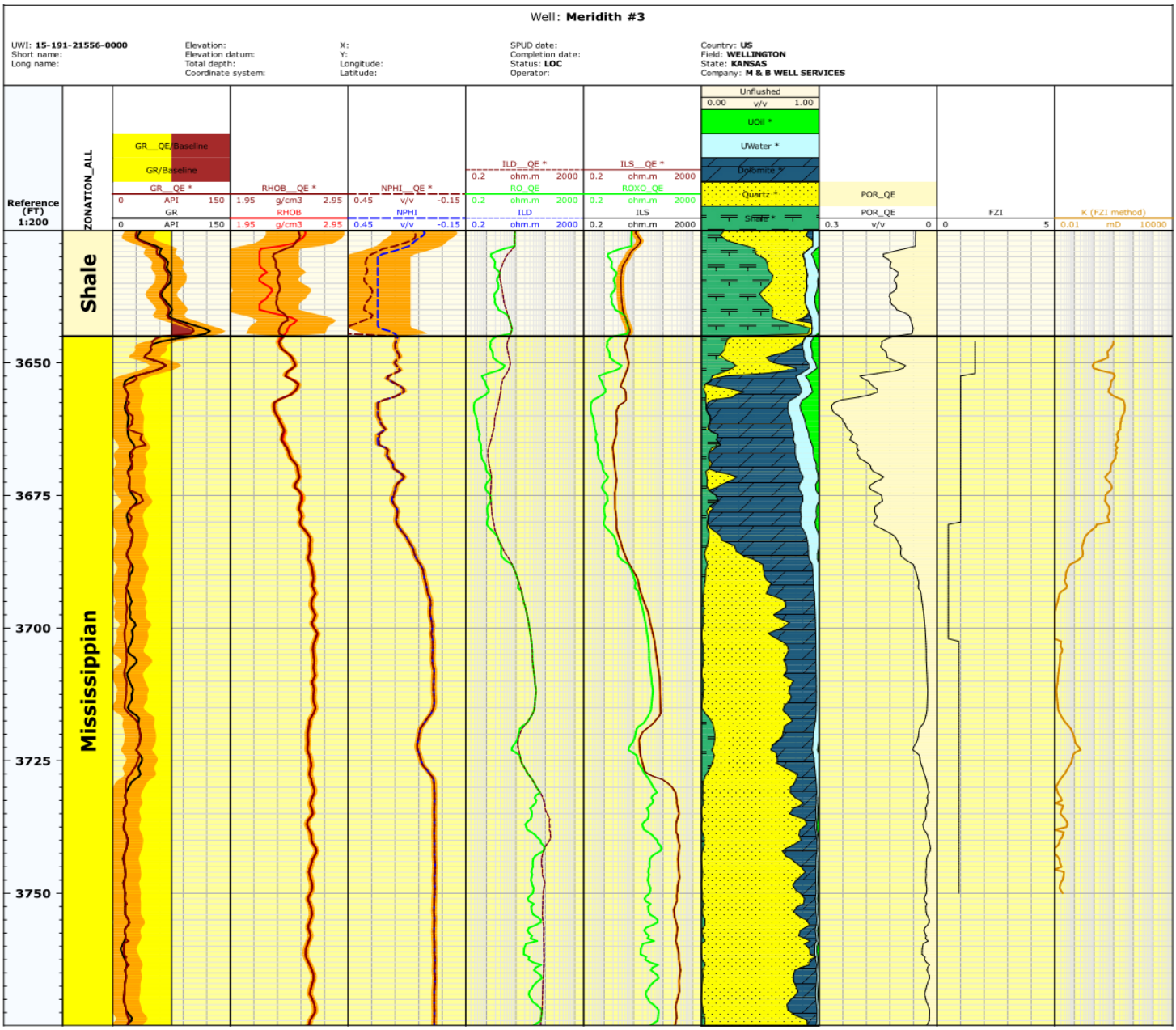

Figure A15: Layout of Meridith #3 showing average FZI in each of six zones and permeability from the FZI-SWP method

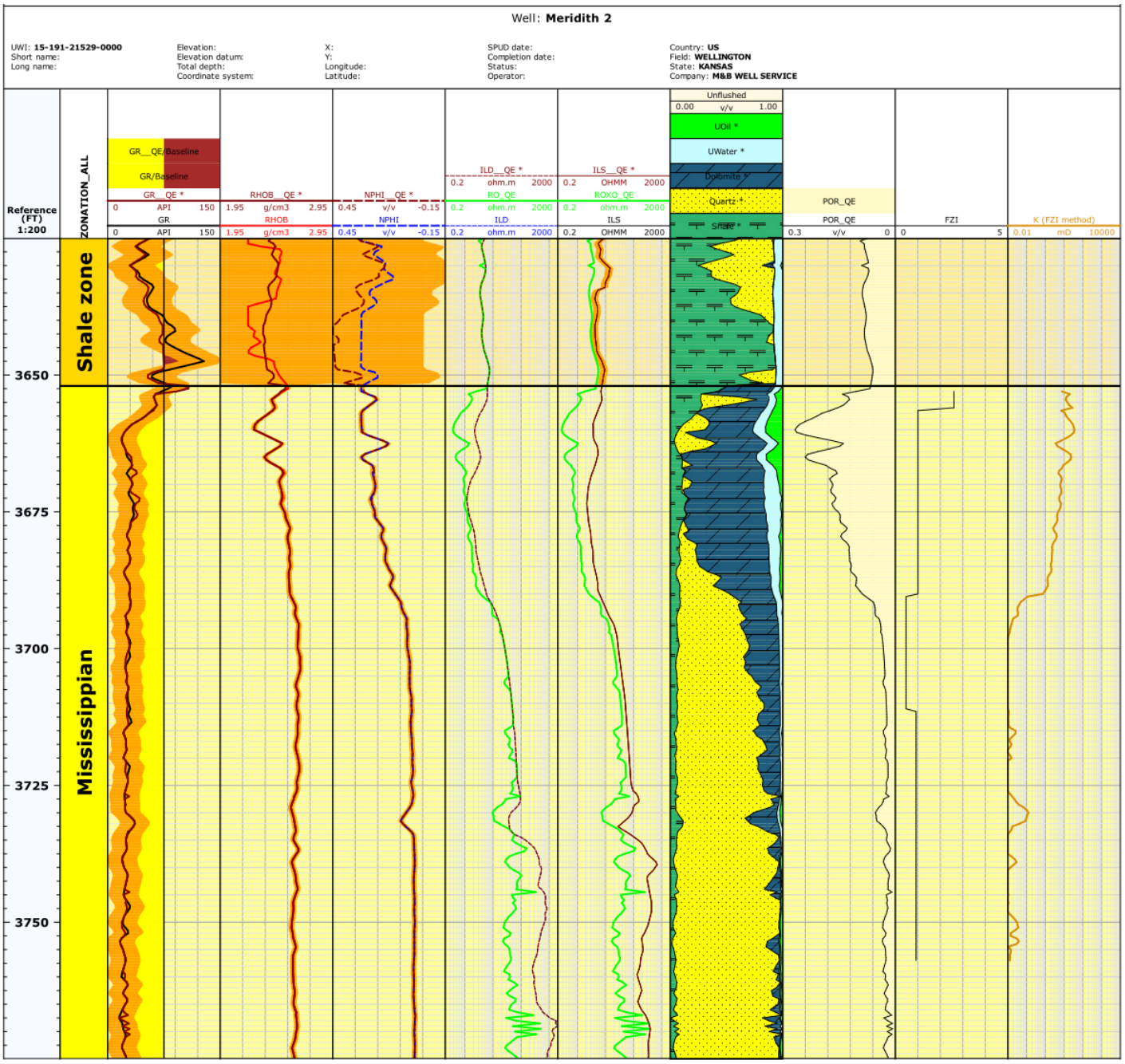

Figure A16: Layout of Meridith #2 showing average FZI in each of six zones and permeability from the FZI-SWP method

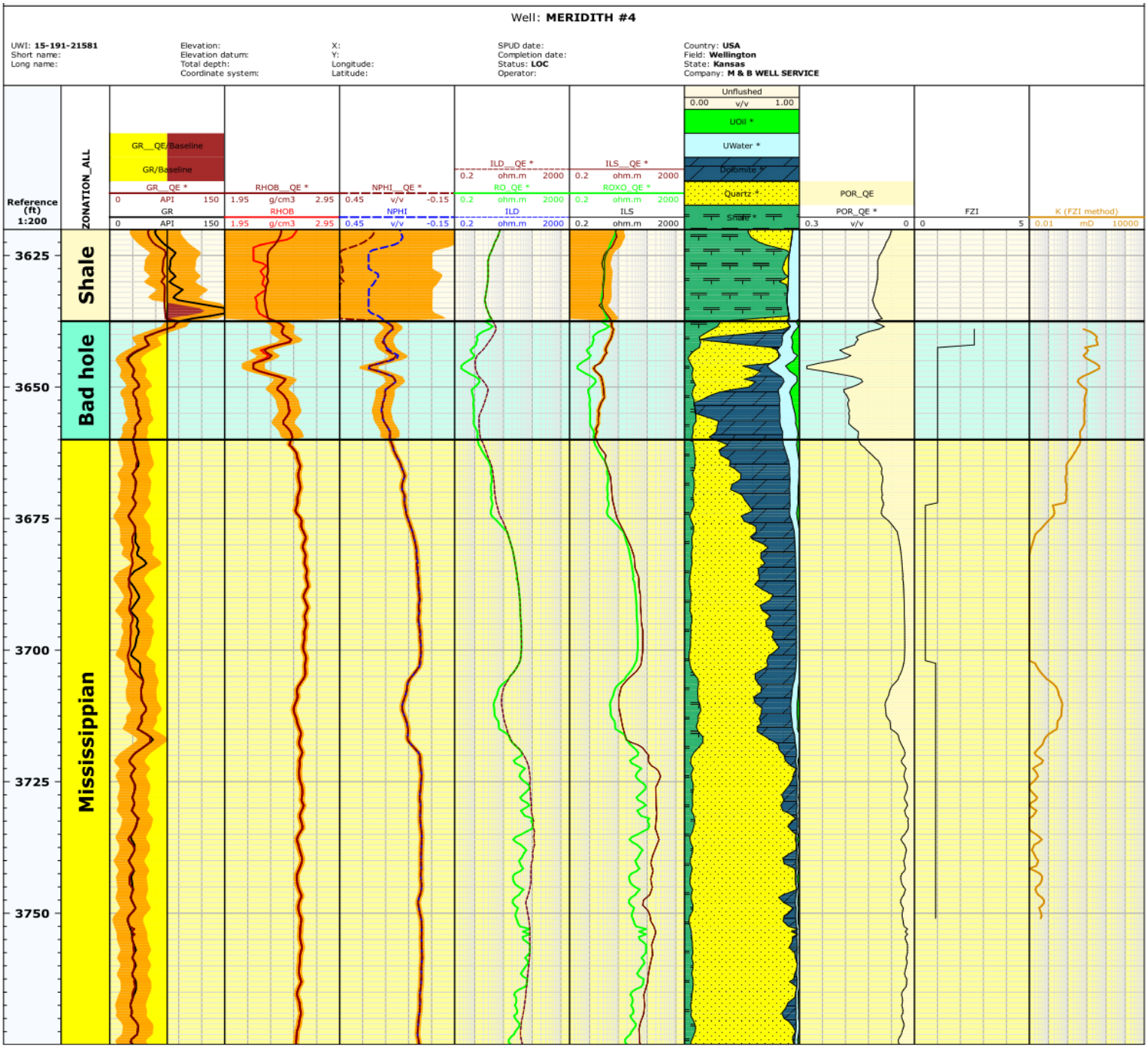

Figure A17: Layout of Meridith #4 showing average FZI in each of six zones and permeability from the FZI-SWP method

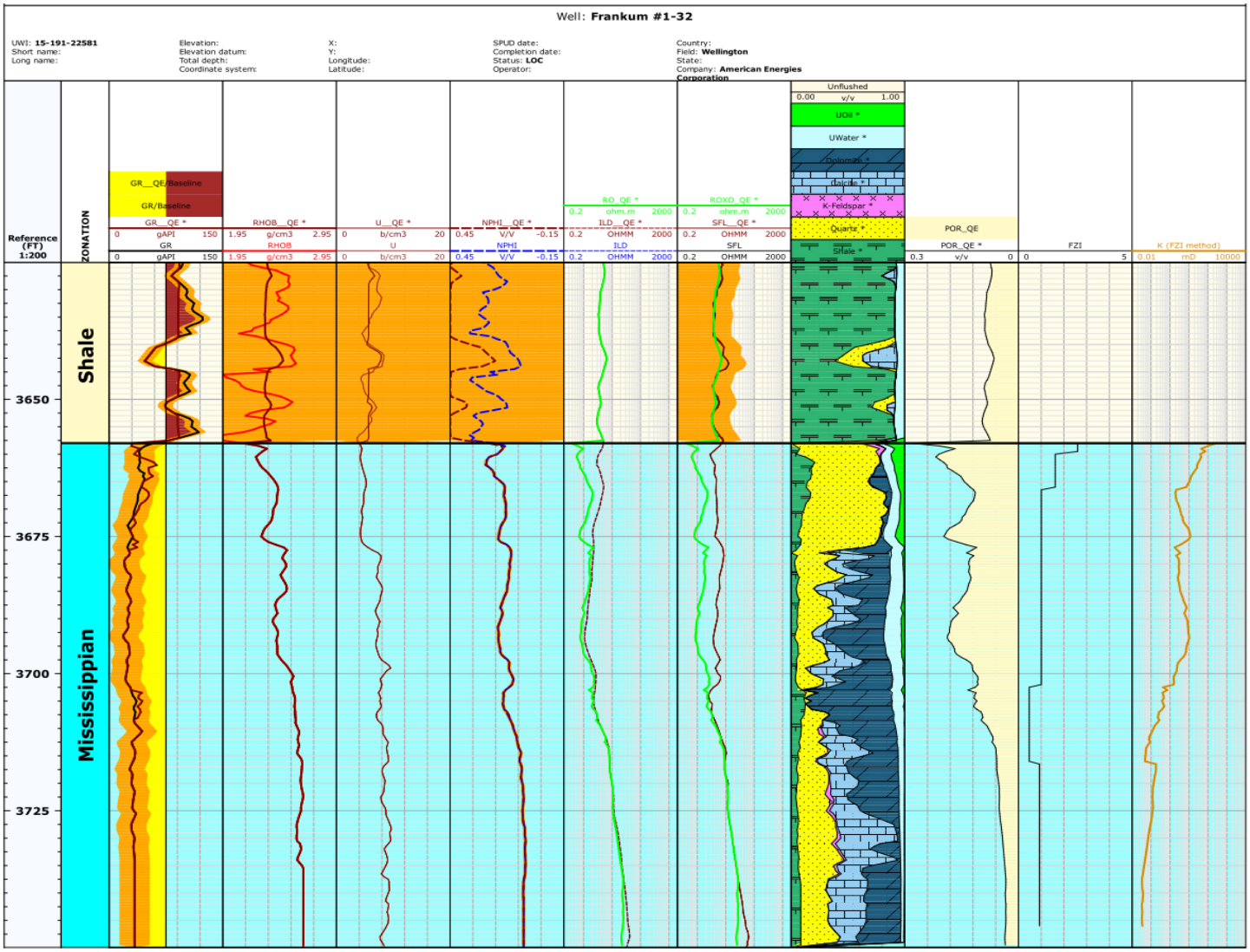

Figure A18: Layout of Frankum # 1-32 showing average FZI in each of six zones and permeability from the FZI-SWP method

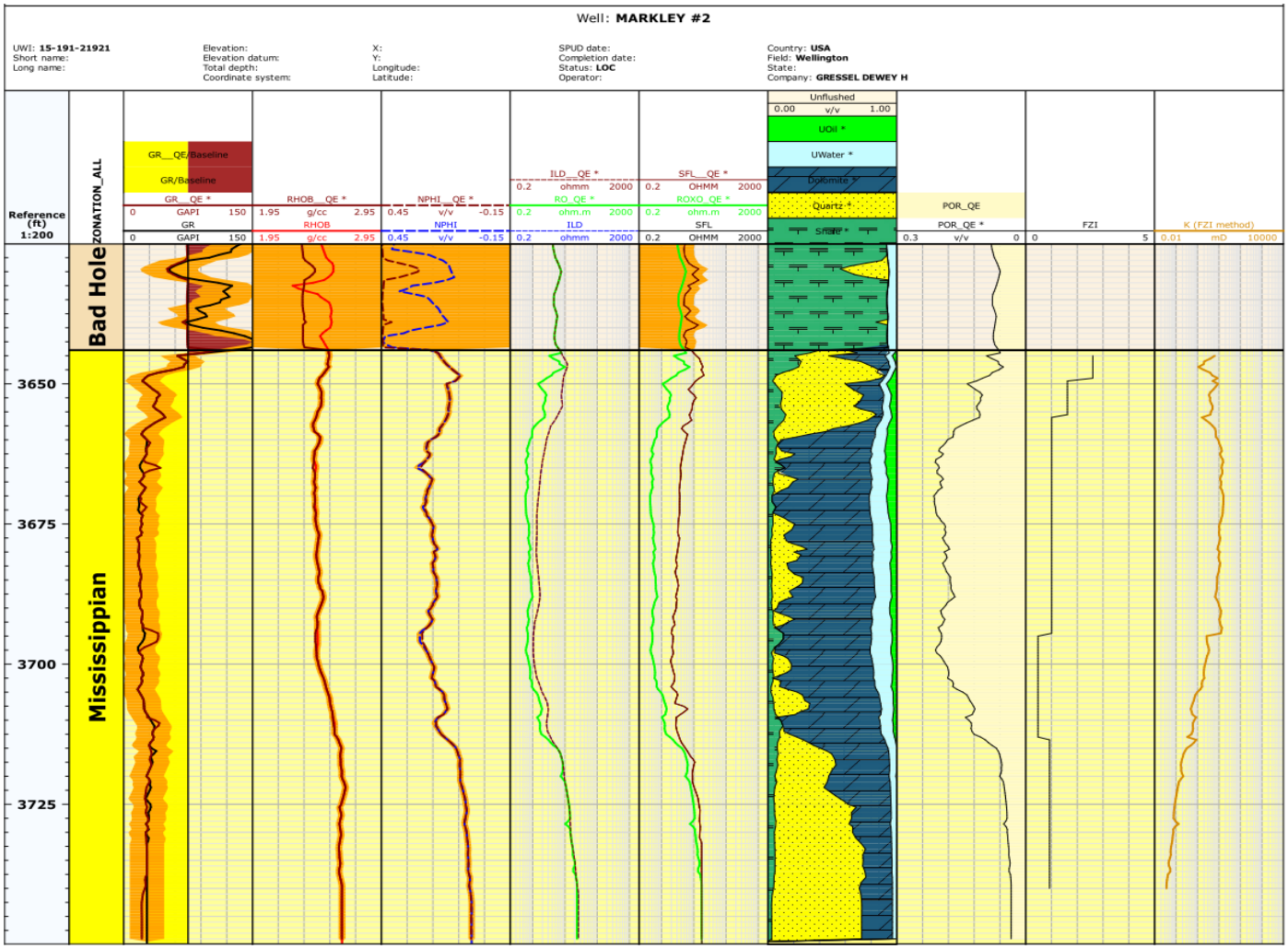

Figure A19: Layout of Markley #2 showing average FZI in each of six zones and permeability from the FZI-SWP method

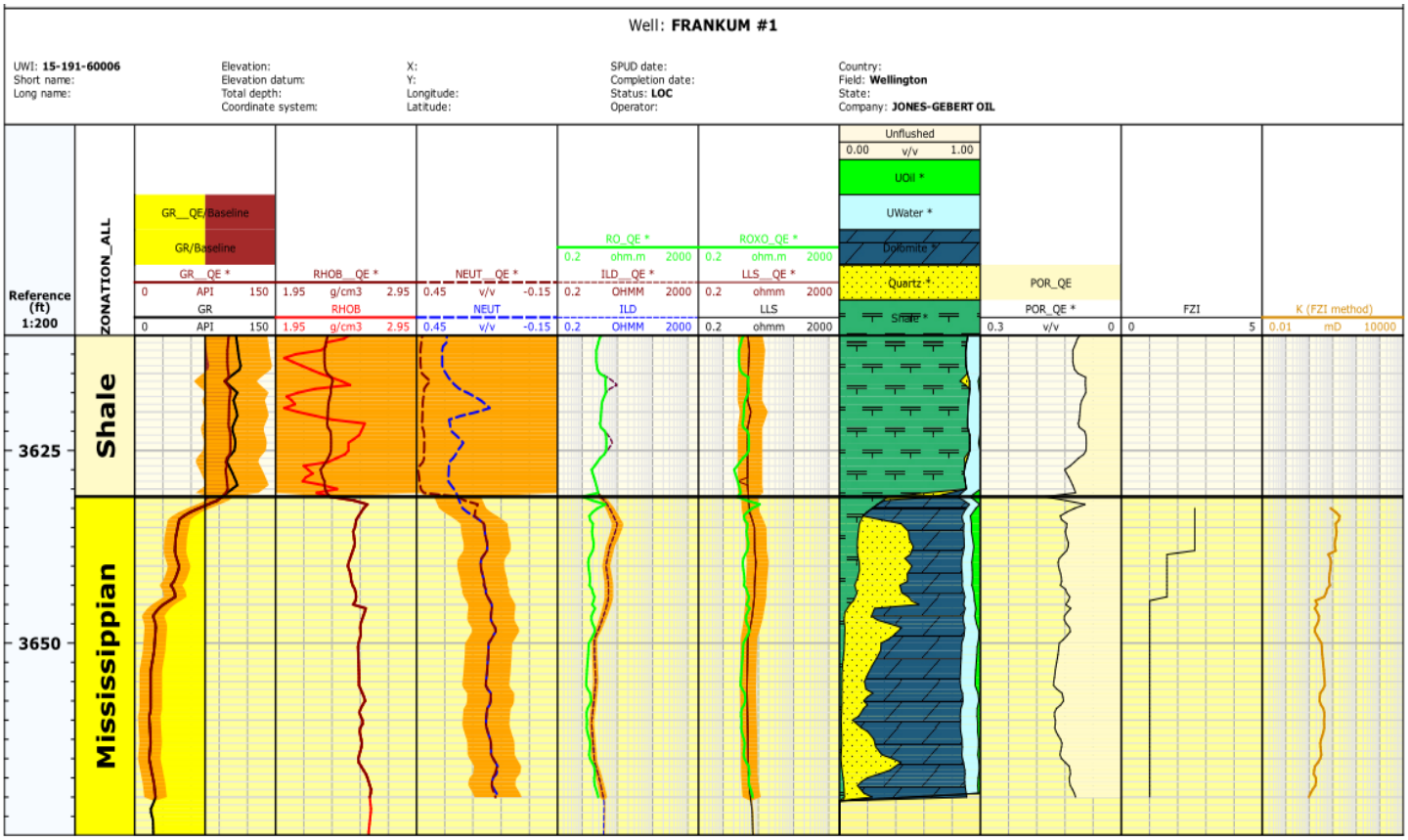

Figure A20: Layout of Frankum #1 showing average FZI in each of six zones and permeability from the FZI-SWP method

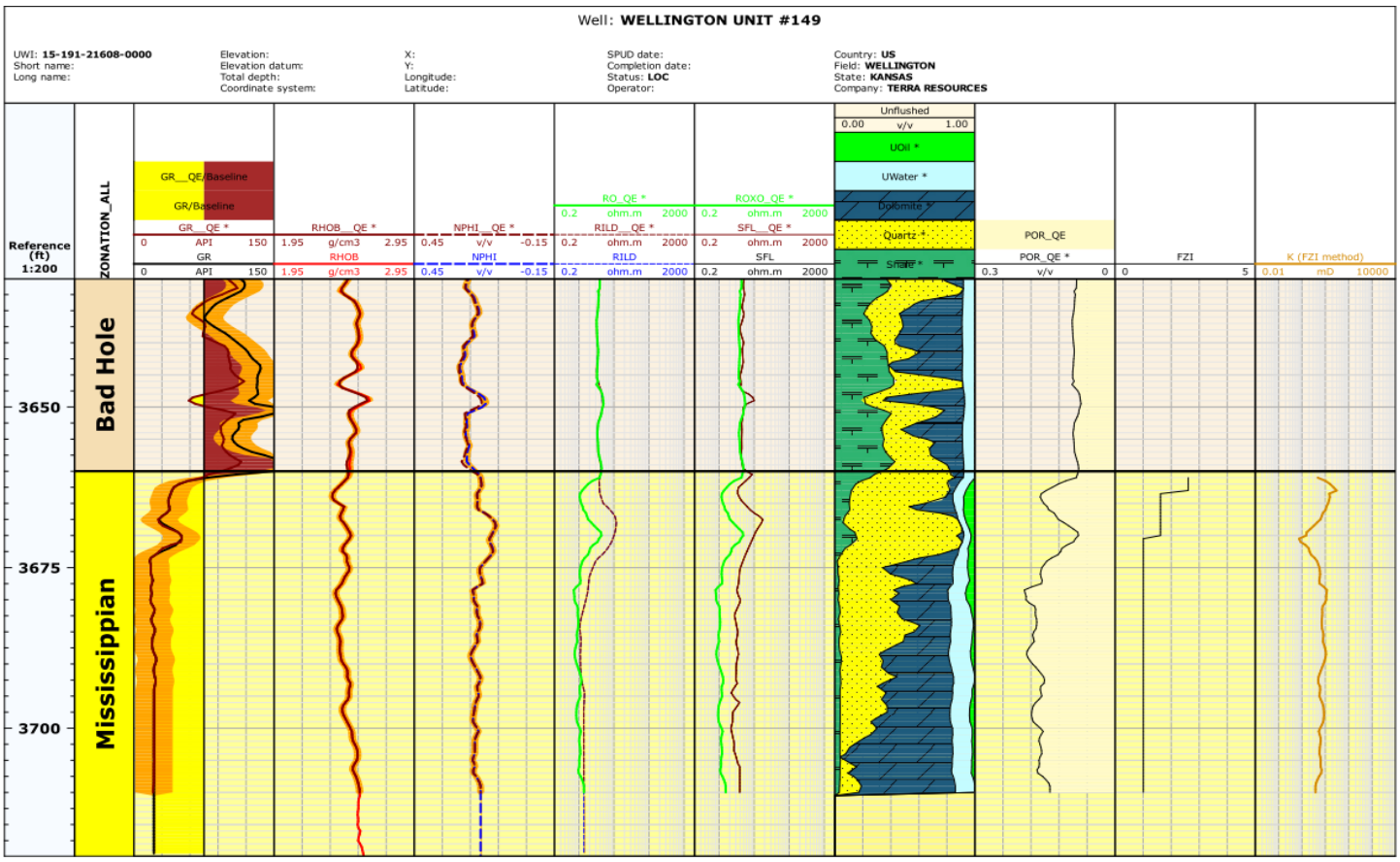

Figure A21: Layout of Well #149 showing average FZI in each of six zones and permeability from the FZI-SWP method

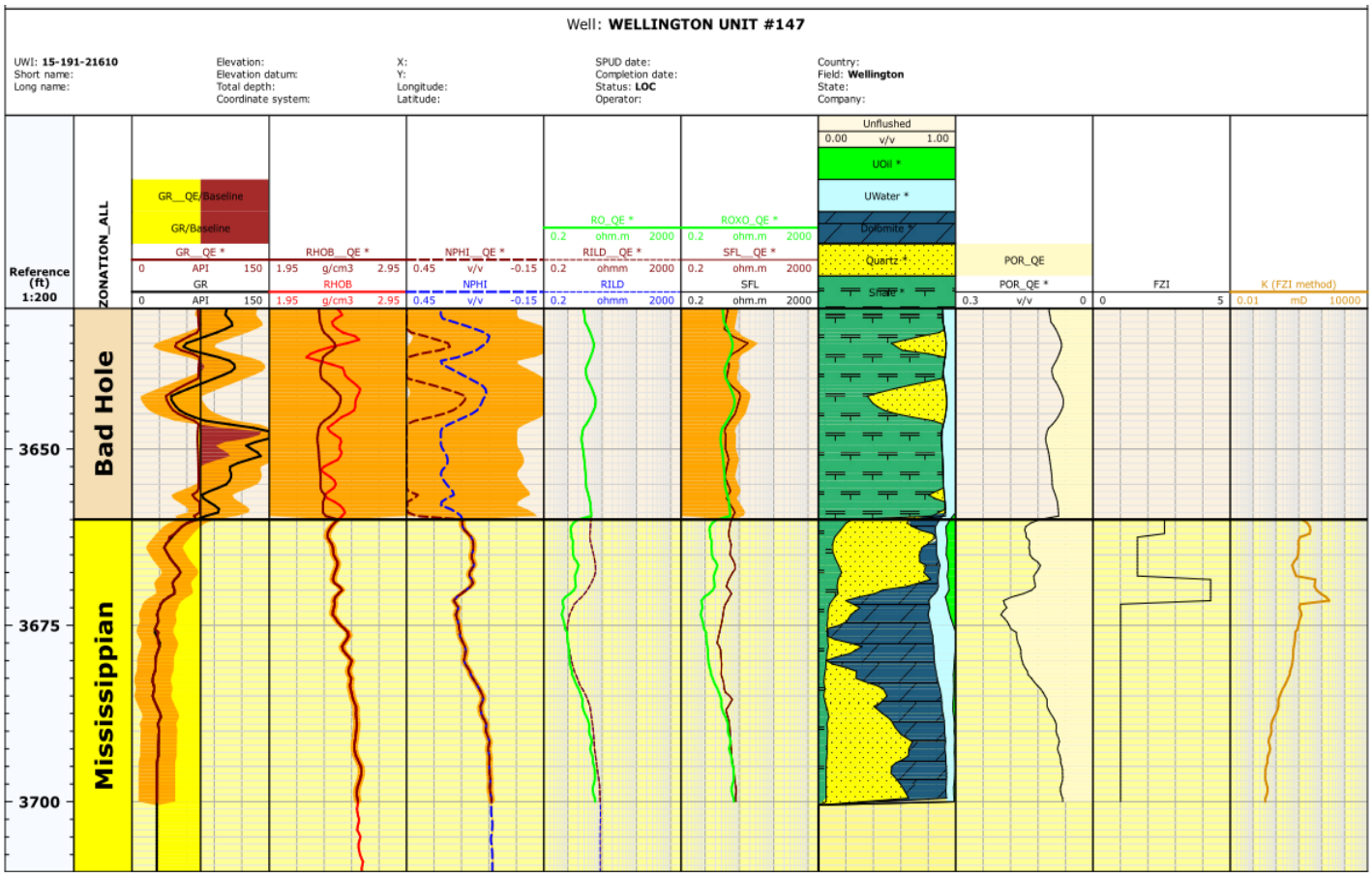

Figure A22: Layout of Well #147 showing average FZI in each of six zones and permeability from the FZI-SWP method

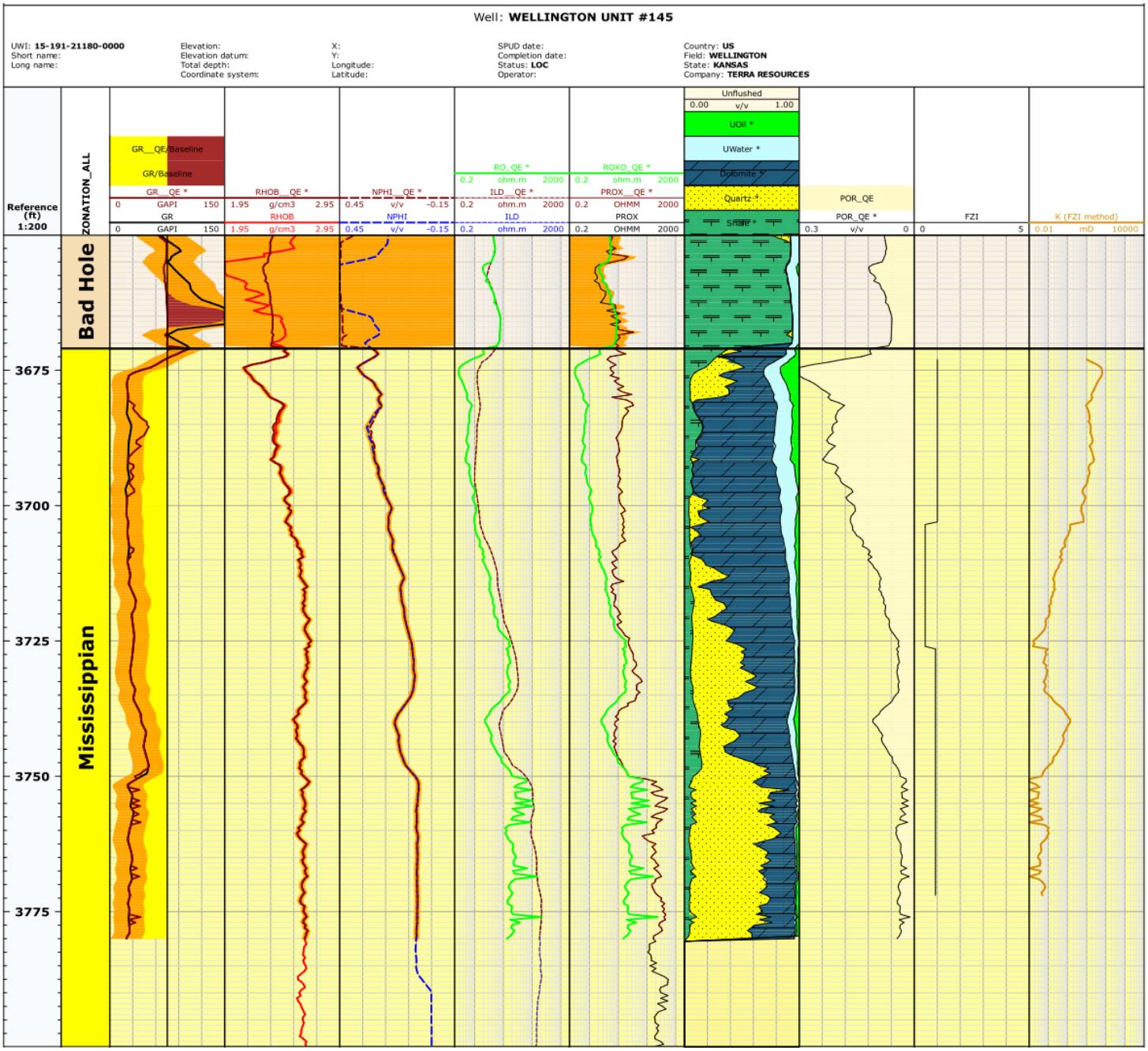

Figure A23: Layout of Well #145 showing average FZI in each of six zones and permeability from the FZI-SWP method

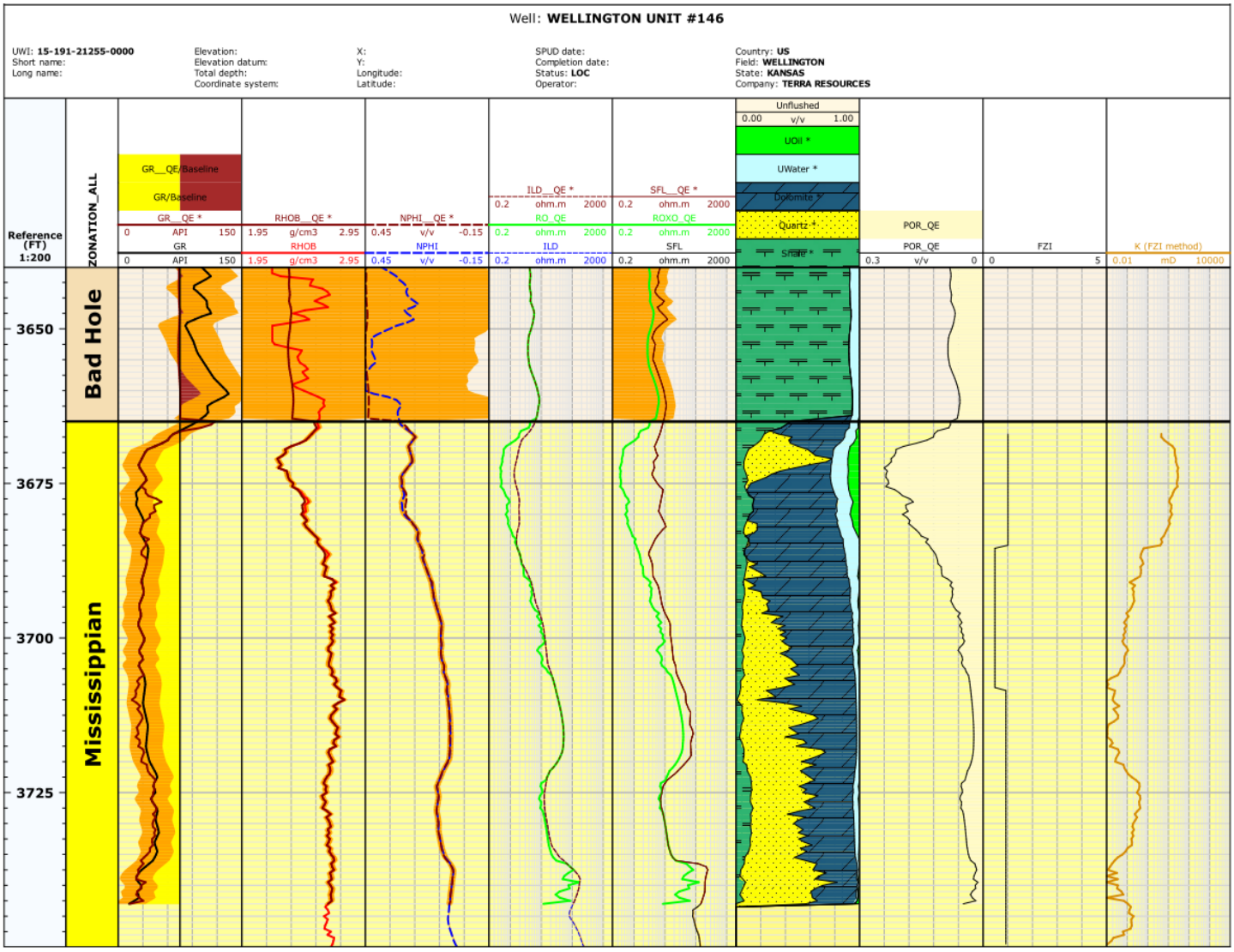

Figure A24: Layout of Well #146 showing average FZI in each of six zones and permeability from the FZI-SWP method

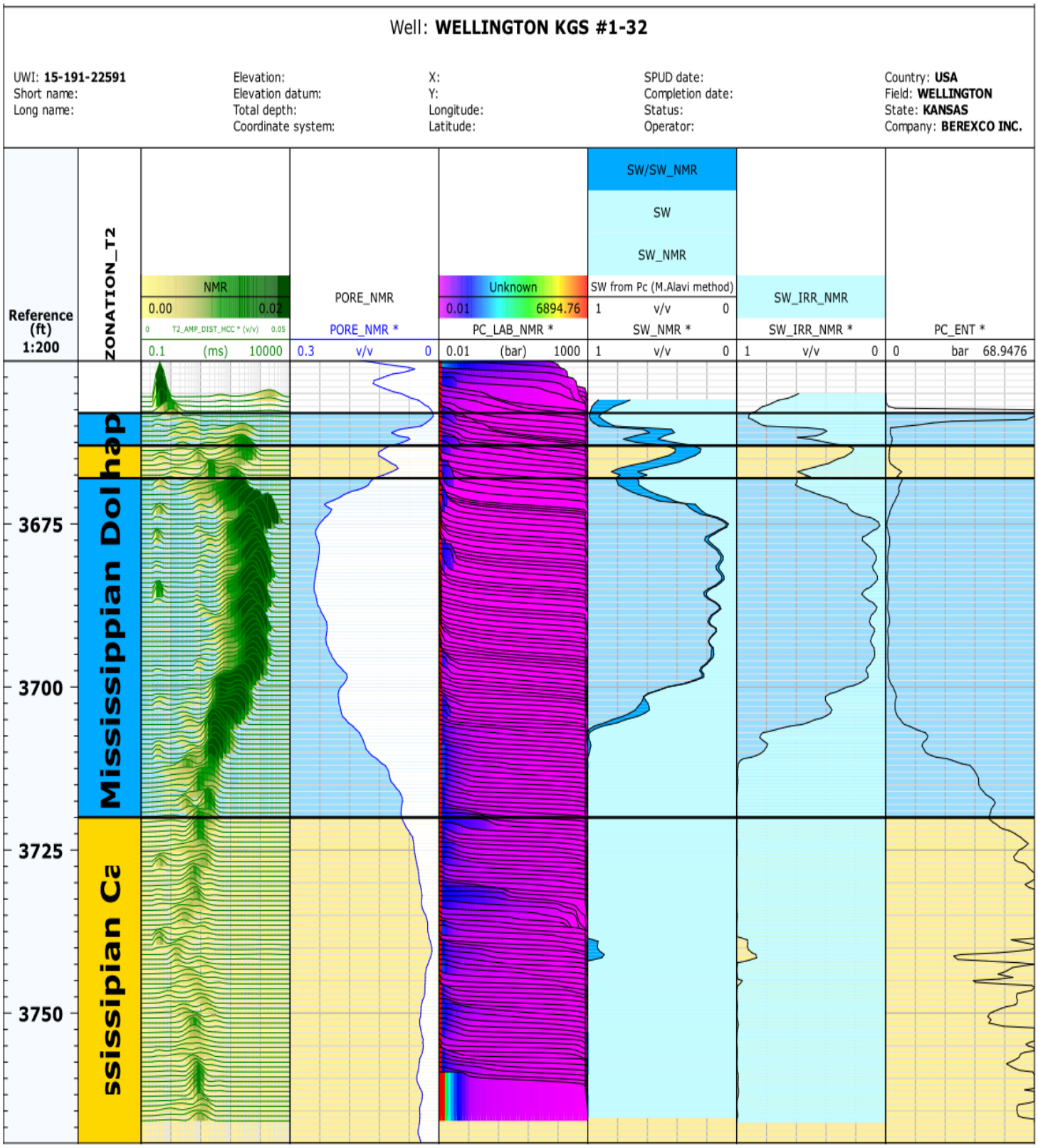

Figure A25: Calculated initial water saturation using the Pc M.F.Alavi method compared with saturation from the NMR log

APPENDIX B. Relative Permeability Chat Section

RQI=			0.320	
Sor	Swc	Chat	Krw max	Kro max
0.321	0.45	1	0.204	0.871
q	1.5		p	2.5
Sw	So	SwD	Krw	kro
0.450	0.550	0.000	0.000	0.871
0.470	0.530	0.087	0.005	0.694
0.490	0.510	0.174	0.015	0.540
0.510	0.490	0.262	0.027	0.408
0.530	0.470	0.349	0.042	0.298
0.550	0.450	0.436	0.059	0.208
0.570	0.430	0.523	0.077	0.137
0.590	0.410	0.610	0.097	0.083
0.610	0.390	0.698	0.119	0.044
0.630	0.370	0.785	0.142	0.019
0.650	0.350	0.872	0.166	0.005
0.670	0.330	0.959	0.191	0.000
0.679	0.321	1.000	0.204	0.000

Table B1: Relative permeability for the chat section at RQI=0.320

RQI=			0.280	
Sor	Swc	Chat	Krw max	Kro max
0.300	0.5	2	0.214	0.869
q	1.5		p	2.5
Sw	So	SwD	Krw	kro
0.500	0.500	0	0	0.869
0.520	0.480	0.1	0.007	0.668
0.540	0.460	0.2	0.019	0.498
0.560	0.440	0.3	0.035	0.356
0.580	0.420	0.4	0.054	0.242
0.600	0.400	0.5	0.075	0.154
0.620	0.380	0.6	0.099	0.088
0.640	0.360	0.7	0.125	0.043
0.660	0.340	0.8	0.153	0.016
0.680	0.320	0.9	0.182	0.003
0.700	0.300	1.0	0.214	0.000

Table B2: Relative permeability for the chat section at RQI=0.280

RQI=			0.245	
Sor	Swc	Chat	Krw max	Kro max
0.270	0.56	3	0.224	0.867
q	1.5		p	2.5
Sw	So	SwD	Krw	kro
0.560	0.440	0.000	0.000	0.867
0.580	0.420	0.118	0.009	0.634
0.600	0.400	0.235	0.026	0.443
0.620	0.380	0.353	0.047	0.292
0.640	0.360	0.471	0.072	0.177
0.660	0.340	0.588	0.101	0.094
0.680	0.320	0.706	0.133	0.041
0.700	0.300	0.824	0.167	0.011
0.720	0.280	0.941	0.204	0.001
0.730	0.270	1.000	0.224	0.000

Table B3: Relative permeability for the chat section at RQI=0.245

RQI=			0.220	
Sor	Swc	Chat	Krw max	Kro max
0.240	0.6	4	0.232	0.865
q	1.5		p	2.5
Sw	So	SwD	Krw	kro
0.600	0.400	0.000	0	0.865
0.620	0.380	0.125	0.010262	0.620
0.640	0.360	0.250	0.029026	0.421
0.660	0.340	0.375	0.053324	0.267
0.680	0.320	0.500	0.082097	0.153
0.700	0.300	0.625	0.114735	0.074
0.720	0.280	0.750	0.150823	0.027
0.740	0.260	0.875	0.190058	0.005
0.760	0.240	1.000	0.232206	0.000

Table B4: Relative permeability for the chat section at RQI=0.220

RQI=			0.200	
Sor	Swc	Chat	Krw max	Kro max
0.210	0.66	5	0.240	0.864
q	1.5		p	2.5
Sw	So	SwD	Krw	kro
0.660	0.340	0.000	0.000	0.864
0.680	0.320	0.154	0.014	0.569
0.700	0.300	0.308	0.041	0.344
0.720	0.280	0.462	0.075	0.184
0.740	0.260	0.615	0.116	0.079
0.760	0.240	0.769	0.162	0.022
0.780	0.220	0.923	0.213	0.001
0.790	0.210	1.000	0.240	0.000

Table B5: Relative permeability for the chat section at RQI=0.200

RQI=			0.175	
Sor	Swc	Chat	Krw max	Kro max
0.155	0.75	6	0.251	0.861
q	1.5		p	2.5
Sw	So	SwD	Krw	kro
0.750	0.250	0	0	0.861
0.770	0.230	0.210526316	0.02429	0.477
0.790	0.210	0.421052632	0.068701	0.220
0.810	0.190	0.631578947	0.126212	0.071
0.830	0.170	0.842105263	0.194317	0.009
0.845	0.155	1	0.251455	0.000

Table B6: Relative permeability for the chat section at RQI=0.175

RQI=			0.145	
Sor	Swc	Chat	Krw max	Kro max
0.090	0.83	7	0.268	0.858
q	1.5		p	2.5
Sw	So	SwD	Krw	kro
0.830	0.170	0	0.000	0.858
0.850	0.150	0.25	0.034	0.418
0.870	0.130	0.5	0.095	0.152
0.890	0.110	0.75	0.174	0.027
0.910	0.090	1	0.268	0.000

Table B7: Relative permeability for the chat section at RQI=0.145

RQI=			0.120	
Sor	Swc	Chat	Krw max	Kro max
0.030	0.930	8	0.287	0.855
q	1.5		p	2.5
Sw	So	SwD	Krw	kro
0.930	0.070	0	0.000	0.855
0.950	0.050	0.5	0.101	0.151
0.970	0.030	1	0.287	0.000

Table B8: Relative permeability for the Ccat section at RQI=0.120

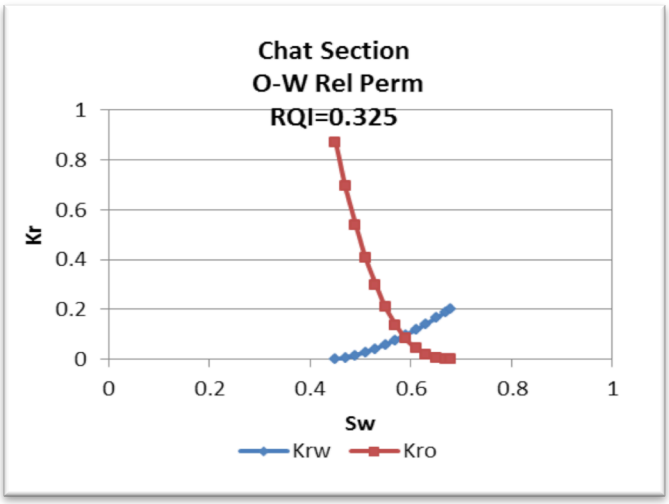

Figure B1: Relative permeability curve for the chat section at RQI=0.325

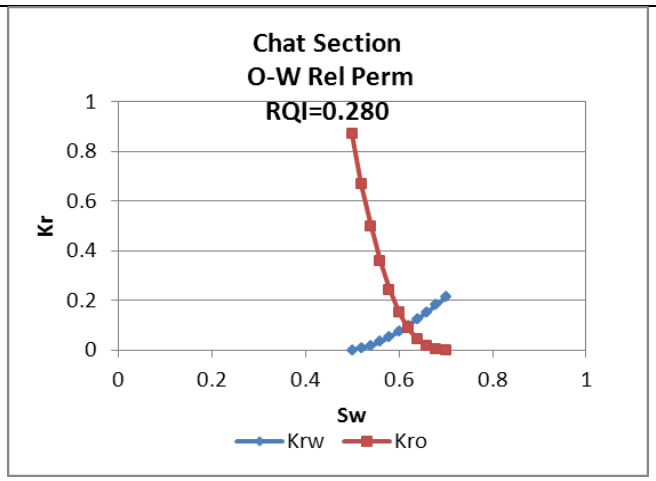

Figure B2: Relative permeability curve for the chat section at RQI=0.280

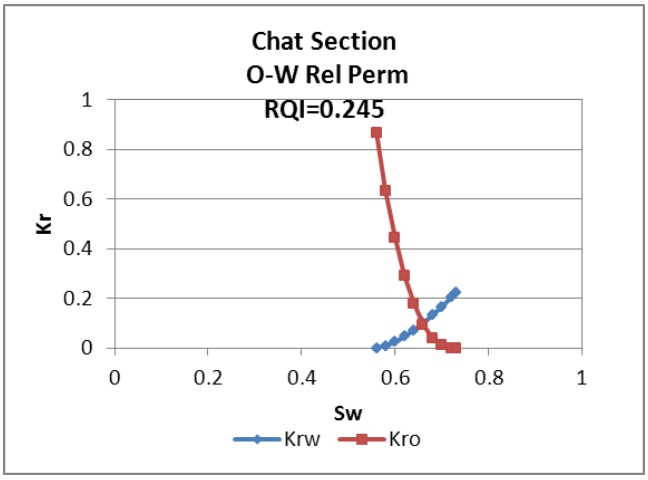

Figure B3: Relative permeability curve for the chat section at RQI=0.245

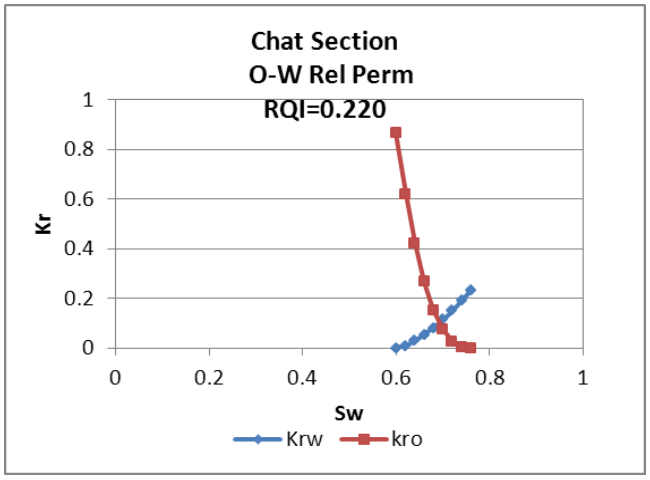

Figure B4: Relative permeability curve for the chat section at RQI=0.220

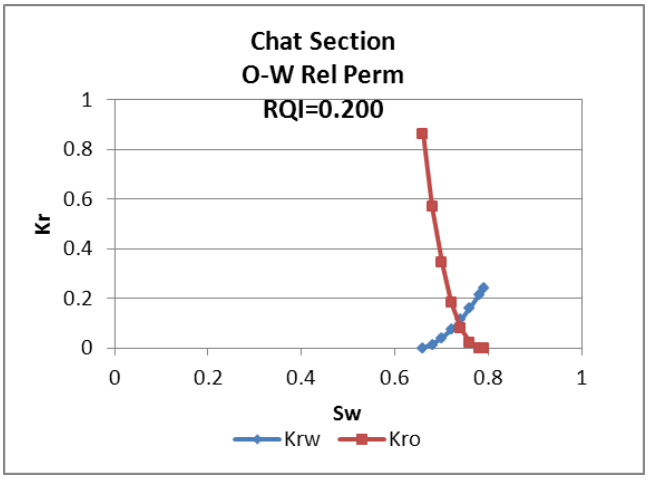

Figure B5: Relative permeability curve for the chat section at RQI=0.200

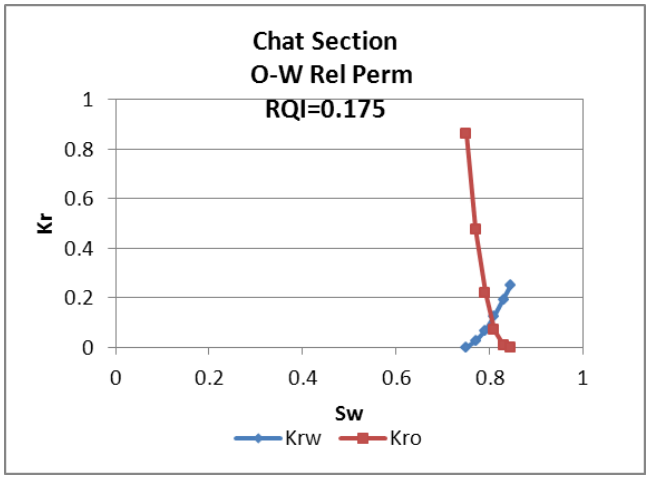

Figure B6: Relative permeability curve for the chat section at RQI=0.175

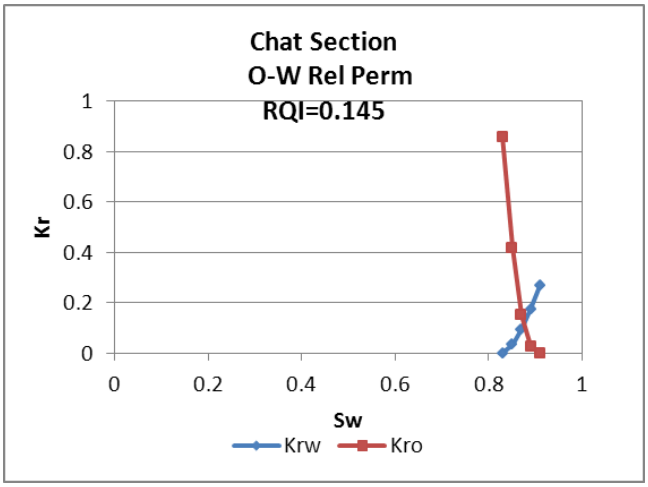

Figure B7: Relative permeability curve for the chat section at RQI=0.145

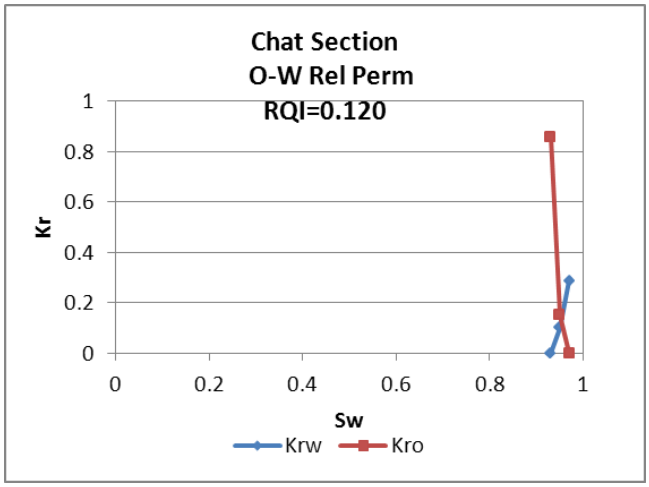

Figure B8: Relative permeability curve for the chat section at RQI=0.120

APPENDIX C. Relative Permeability Carbonate Section

Table C1: Relative permeability table for the carbonate section at RQI=0.520

RQI=			0.520	
Sor	Swc	Carbonate	Krw max	Kro max
0.364	0.08	1	0.172	0.880
q	1.5		p	2.5
Sw	So	SwD	Krw	kro
0.080	0.920	0.000	0	0.880
0.100	0.900	0.036	0.001	0.803
0.120	0.880	0.072	0.003	0.730
0.140	0.860	0.108	0.006	0.661
0.160	0.840	0.144	0.009	0.597
0.180	0.820	0.180	0.013	0.536
0.200	0.800	0.216	0.017	0.479
0.220	0.780	0.252	0.022	0.426
0.240	0.760	0.288	0.027	0.377
0.260	0.740	0.324	0.032	0.331
0.280	0.720	0.359	0.037	0.289
0.300	0.700	0.395	0.043	0.250
0.320	0.680	0.431	0.049	0.215
0.340	0.660	0.467	0.055	0.182
0.360	0.640	0.503	0.061	0.153
0.380	0.620	0.539	0.068	0.127
0.400	0.600	0.575	0.075	0.104
0.420	0.580	0.611	0.082	0.083
0.440	0.560	0.647	0.090	0.065
0.460	0.540	0.683	0.097	0.050
0.480	0.520	0.72	0.105	0.037
0.500	0.500	0.755	0.113	0.026
0.520	0.480	0.791	0.121	0.018
0.540	0.460	0.827	0.129	0.011
0.560	0.440	0.863	0.138	0.006
0.580	0.420	0.899	0.147	0.003
0.600	0.400	0.935	0.156	0.001
0.620	0.380	0.971	0.165	0.0001

Table C2: Relative permeability table for the carbonate section at RQI=0.380

RQI=			0.380	
Sor	Swc	Carbonate	Krw max	Kro max
0.342	0.11	2	0.192	0.874
q	1.5		p	2.5
Sw	So	SwD	Krw	kro
0.110	0.890	0.000	0	0.874
0.130	0.870	0.037	0.001	0.797
0.150	0.850	0.073	0.004	0.723
0.170	0.830	0.110	0.007	0.654
0.190	0.810	0.146	0.011	0.589
0.210	0.790	0.183	0.015	0.528
0.230	0.770	0.219	0.020	0.471
0.250	0.750	0.256	0.025	0.418
0.270	0.730	0.292	0.030	0.369
0.290	0.710	0.329	0.036	0.323
0.310	0.690	0.365	0.042	0.281
0.330	0.670	0.402	0.049	0.242
0.350	0.650	0.438	0.056	0.207
0.370	0.630	0.475	0.063	0.175
0.390	0.610	0.511	0.070	0.146
0.410	0.590	0.548	0.078	0.120
0.430	0.570	0.584	0.086	0.097
0.450	0.550	0.621	0.094	0.077
0.470	0.530	0.657	0.102	0.060
0.490	0.510	0.694	0.111	0.045
0.510	0.490	0.73	0.120	0.033
0.530	0.470	0.767	0.129	0.023
0.550	0.450	0.803	0.138	0.015
0.570	0.430	0.840	0.148	0.009
0.590	0.410	0.876	0.157	0.005
0.610	0.390	0.913	0.167	0.002
0.630	0.370	0.949	0.178	0.001
0.650	0.350	0.986	0.188	0.00002
0.658	0.342	1.000	0.192	0.000

Table C3: Relative permeability table for the carbonate section at RQI=0.250

RQI=			0.250	
Sor	Swc	Carbonate	Krw max	Kro max
0.315	0.15	3	0.222	0.867
q	1.5		p	2.5
Sw	So	SwD	Krw	kro
0.150	0.850	0.000	0	0.867
0.170	0.830	0.037	0.002	0.789
0.190	0.810	0.075	0.005	0.714
0.210	0.790	0.112	0.008	0.644
0.230	0.770	0.149	0.013	0.579
0.250	0.750	0.187	0.018	0.517
0.270	0.730	0.224	0.024	0.460
0.290	0.710	0.261	0.030	0.406
0.310	0.690	0.299	0.036	0.357
0.330	0.670	0.336	0.043	0.311
0.350	0.650	0.374	0.051	0.269
0.370	0.630	0.411	0.059	0.231
0.390	0.610	0.448	0.067	0.196
0.410	0.590	0.486	0.075	0.165
0.430	0.570	0.523	0.084	0.136
0.450	0.550	0.560	0.093	0.111
0.470	0.530	0.598	0.103	0.089
0.490	0.510	0.635	0.112	0.070
0.510	0.490	0.672	0.122	0.053
0.530	0.470	0.710	0.133	0.039
0.550	0.450	0.75	0.143	0.028
0.570	0.430	0.784	0.154	0.019
0.590	0.410	0.822	0.165	0.012
0.610	0.390	0.859	0.177	0.006
0.630	0.370	0.897	0.189	0.003
0.650	0.350	0.934	0.200	0.001
0.670	0.330	0.971	0.213	0.0001
0.685	0.315	1.000	0.222	0.0000

Table C4: Relative permeability table for the carbonate section at RQI=0.160

RQI=			0.160	
Sor	Swc	Carbonate	Krw max	Kro max
0.278	0.22	4	0.259	0.860
q	1.5		p	2.5
Sw	So	SwD	Krw	kro
0.220	0.780	0.000	0	0.860
0.240	0.760	0.040	0.002	0.777
0.260	0.740	0.080	0.006	0.699
0.280	0.720	0.120	0.011	0.625
0.300	0.700	0.159	0.017	0.557
0.320	0.680	0.199	0.023	0.493
0.340	0.660	0.239	0.030	0.434
0.360	0.640	0.279	0.038	0.380
0.380	0.620	0.319	0.047	0.329
0.400	0.600	0.359	0.056	0.283
0.420	0.580	0.399	0.065	0.241
0.440	0.560	0.438	0.075	0.203
0.460	0.540	0.478	0.086	0.169
0.480	0.520	0.518	0.097	0.139
0.500	0.500	0.558	0.108	0.112
0.520	0.480	0.598	0.120	0.088
0.540	0.460	0.638	0.132	0.068
0.560	0.440	0.677	0.145	0.051
0.580	0.420	0.717	0.158	0.037
0.600	0.400	0.757	0.171	0.025
0.620	0.380	0.80	0.185	0.016
0.640	0.360	0.837	0.199	0.009
0.660	0.340	0.877	0.213	0.005
0.680	0.320	0.917	0.228	0.002
0.700	0.300	0.956	0.243	0.00034
0.720	0.280	0.996	0.258	0.00000
0.722	0.278	1.000	0.259	0.000

Table C5: Relative permeability table for the carbonate section at RQI=0.100

RQI=			0.100	
Sor	Swc	Carbonate	Krw max	Kro max
0.250	0.315	5	0.306	0.852
q	1.5		p	2.5
Sw	So	SwD	Krw	kro
0.315	0.685	0.000	0	0.852
0.335	0.665	0.046	0.003	0.757
0.355	0.645	0.092	0.009	0.669
0.375	0.625	0.138	0.016	0.588
0.395	0.605	0.184	0.024	0.512
0.415	0.585	0.230	0.034	0.443
0.435	0.565	0.276	0.044	0.380
0.455	0.545	0.322	0.056	0.322
0.475	0.525	0.368	0.068	0.270
0.495	0.505	0.414	0.081	0.224
0.515	0.485	0.460	0.095	0.182
0.535	0.465	0.506	0.110	0.146
0.555	0.445	0.552	0.125	0.114
0.575	0.425	0.598	0.141	0.087
0.595	0.405	0.644	0.158	0.064
0.615	0.385	0.690	0.175	0.046
0.635	0.365	0.736	0.193	0.030
0.655	0.345	0.782	0.211	0.019
0.675	0.325	0.828	0.230	0.010
0.695	0.305	0.874	0.250	0.005
0.715	0.285	0.92	0.270	0.002
0.735	0.265	0.966	0.290	0.000
0.750	0.250	1.000	0.306	0.000

Table C6: Relative permeability table for the carbonate section at RQI=0.080

RQI=			0.080	
Sor	Swc	Carbonate	Krw max	Kro max
0.220	0.43	6	0.330	0.848
q	1.5		p	2.5
Sw	So	SwD	Krw	kro
0.430	0.570	0.000	0	0.848
0.450	0.550	0.057	0.005	0.732
0.470	0.530	0.114	0.013	0.626
0.490	0.510	0.171	0.023	0.530
0.510	0.490	0.228	0.036	0.444
0.530	0.470	0.285	0.050	0.366
0.550	0.450	0.343	0.066	0.297
0.570	0.430	0.400	0.083	0.237
0.590	0.410	0.457	0.102	0.184
0.610	0.390	0.514	0.122	0.140
0.630	0.370	0.571	0.142	0.102
0.650	0.350	0.628	0.164	0.072
0.670	0.330	0.685	0.187	0.047
0.690	0.310	0.742	0.211	0.029
0.710	0.290	0.799	0.236	0.015
0.730	0.270	0.856	0.262	0.007
0.750	0.250	0.914	0.288	0.002
0.770	0.230	0.971	0.316	0.0001
0.780	0.220	1.000	0.330	0.000

Table C7: Relative permeability table for the carbonate section at RQI=0.060

RQI=			0.060	
Sor	Swc	Carbonate	Krw max	Kro max
0.200	0.52	7	0.365	0.844
q	1.5		p	2.5
Sw	So	SwD	Krw	kro
0.520	0.480	0.000	0	0.844
0.540	0.460	0.071	0.007	0.701
0.560	0.440	0.143	0.020	0.574
0.580	0.420	0.214	0.036	0.462
0.600	0.400	0.285	0.056	0.364
0.620	0.380	0.357	0.078	0.280
0.640	0.360	0.428	0.102	0.209
0.660	0.340	0.499	0.129	0.150
0.680	0.320	0.571	0.157	0.102
0.700	0.300	0.642	0.188	0.065
0.720	0.280	0.714	0.220	0.037
0.740	0.260	0.785	0.254	0.018
0.760	0.240	0.856	0.289	0.007
0.780	0.220	0.928	0.326	0.001
0.800	0.200	0.999	0.36438	0.000

Table C8: Relative permeability table for the carbonate section at RQI=0.050

RQI=			0.050	
Sor	Swc	Carbonate	Krw max	Kro max
0.174	0.660	8	0.389	0.841
q	1.5		p	2.5
Sw	So	SwD	Krw	kro
0.660	0.340	0.000	0	0.841
0.680	0.320	0.121	0.016	0.609
0.700	0.300	0.242	0.046	0.421
0.720	0.280	0.363	0.085	0.273
0.740	0.260	0.483	0.131	0.161
0.760	0.240	0.604	0.183	0.083
0.780	0.220	0.725	0.240	0.033
0.800	0.200	0.846	0.303	0.008
0.820	0.180	0.967	0.370	0.000
0.826	0.174	1.000	0.389	0.000

Figure C1: Relative permeability curve for the carbonate section at RQI=0.520

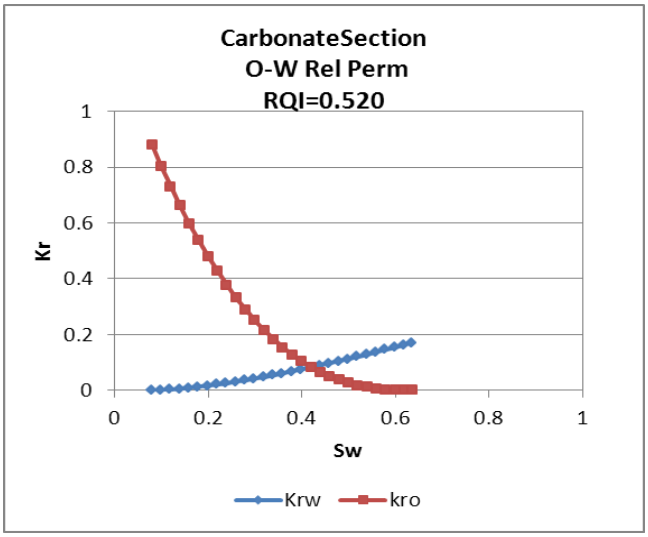

Figure C2: Relative permeability curve for the carbonate section at RQI=0.380

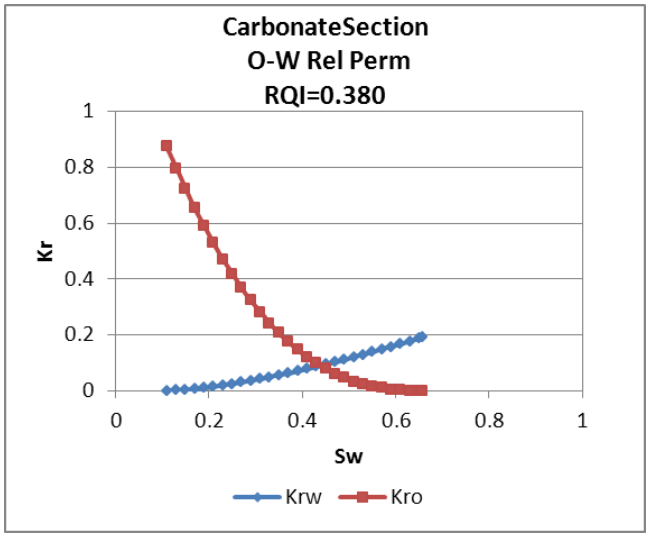

Figure C3: Relative permeability curve for the carbonate section at RQI=0.25

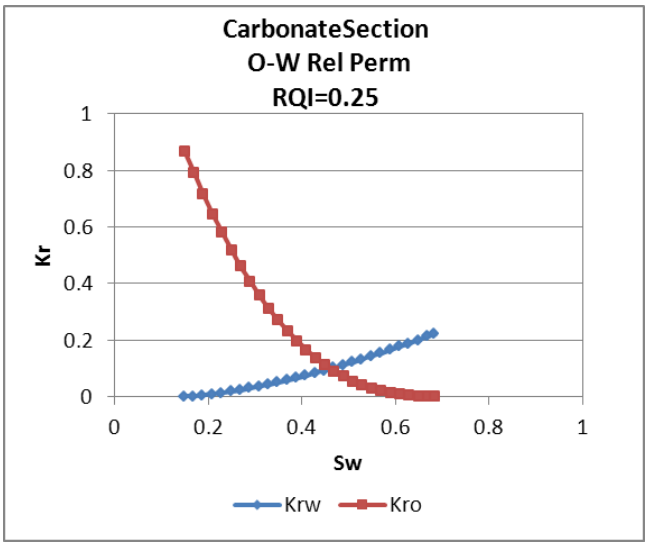

Figure C4: Relative permeability curve for the carbonate section at RQI=0.16

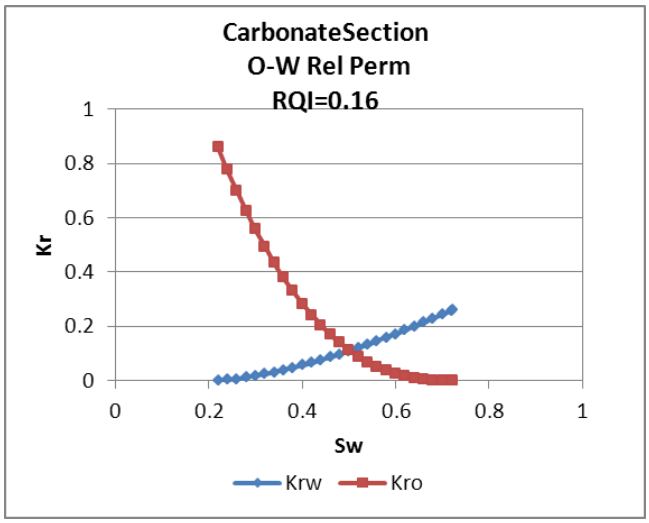

Figure C5:Relative permeability curve for the carbonate section at RQI=0.100

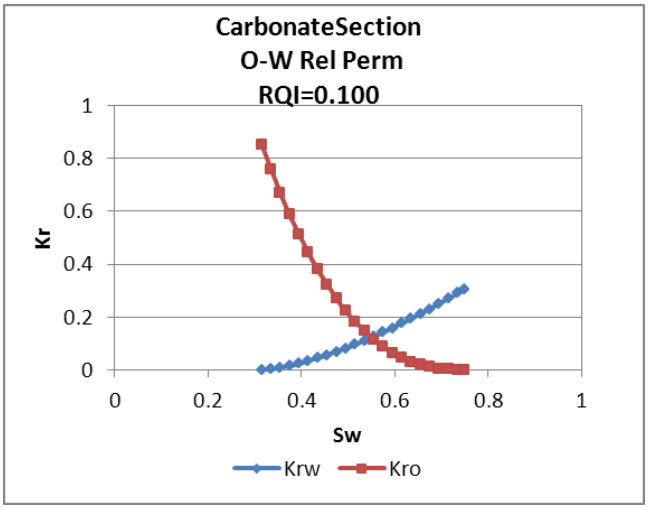

Figure C6: Relative permeability curve for the carbonate section at RQI=0.08

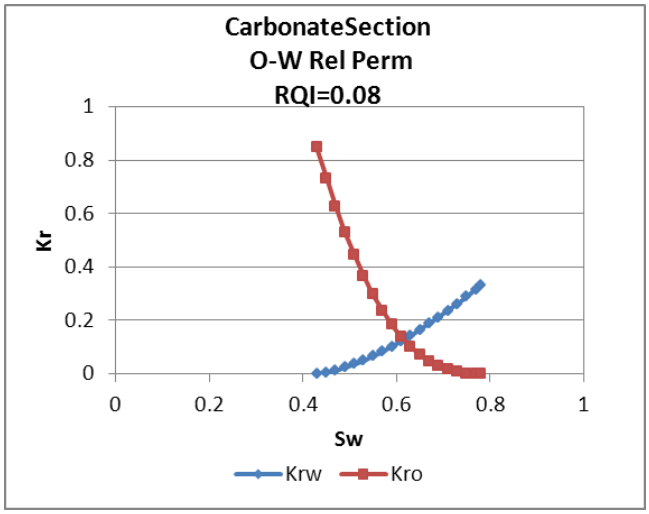

Figure C7: Relative permeability curve for the carbonate section at RQI=0.06

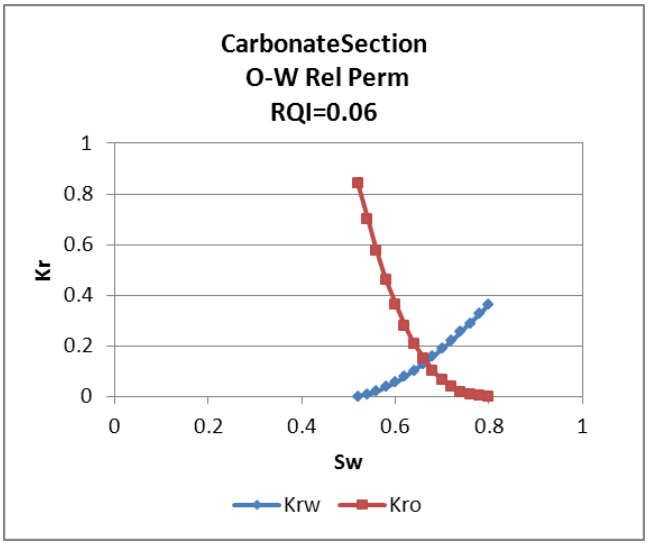

Figure C8: Relative permeability curve for the carbonate section at RQI=0.05